THE COMPLEX OF 2-AMINOTHIOPHENOL LIGAND WITH PLATINUM: A NOVEL PLATINUM BLUES CONTAINING SULFUR DONOR LIGAND

A THESIS SUBMITTED TO
THE GRADUATE SCHOOL OF NATURAL AND APPLIED SCIENCES
OF
MIDDLE EAST TECHNICAL UNIVERSITY

BY

İSMAİL ERİLHAN

IN PARTIAL FULFILLMENT OF THE REQUIREMENTS
FOR
THE DEGREE OF MASTER OF SCIENCE
IN
DEPARTMENT OF CHEMISTRY

JUNE 2007

I hereby declare that all information in this document has been obtained and presented in accordance with academic rules and ethical conduct. I also declare that, as required by these rules and conduct, I have fully cited and referenced all material and results that are not original to this work.

Name, Last name :

Signature :

ABSTRACT

COMPLEX OF 2-AMINOTHIOPHENOL
LIGAND WITH PLATINUM:
A NOVEL PLATINUM BLUES
CONTAINING SULFUR DONOR LIGAND

Erilhan, İsmail

M.S. Department of Chemistry

Supervisor: Prof. Dr. Hüseyin İşçi

Co-supervisor: Assoc. Prof. Dr. Şeniz Özalp Yaman

June 2007, 68 pages

The reaction of K_2PtCl_4 with 2-aminothiophenol (H2-atp), $C_6H_5(SH)(NH_2)$, yielded a dark blue solid product. This work is about the characterization of this dark blue solid and the investigation of its binding interaction to DNA and enzyme activity.

The blue solid product or the "blue complex" (as we called it in this work) is soluble in acetone, acetonitrile and DMSO yielding a blue solution. It is stable in solution and has a very strong absorption band at 724 nm (molar absorptivity in acetone is 57782 $M^{-1}cm^{-1}$ per mole of platinum).

The product is paramagnetic and displays one kind of platinum in XPS (platinum $4f_{7/2}$ and $4f_{5/2}$ binding energies were obtained at 71.1 and 74.6 eV, respectively). The elemental (C, H, N, S, Pt) analysis indicated that the platinum to ligand (2-aminothiophenolate) mole ratio is 1:2. The interpretation of the data collected from elemental analysis and ESR, XPS, ^{1}H-, ^{13}C-, ^{195}Pt-NMR, CV measurements leads to conclude that the blue complex prepared in this work is a new platinum blues with a formula $[Pt^{III}Pt_3^{II}(2\text{-atp})_8(OH)(H_2O)]$, where 2-atp is 2-aminothiophenolate ligand. This is the first example of platinum blues, in which the bridging ligand is a nitrogen and sulfur donor one. The proposed structure can be visualized as a dimer of binuclear head-to-head isomer of $[Pt_2^{II}(2\text{-atp})_4]$, with C_{2h} symmetry. The band at 724 nm is assigned to an allowed electronic transition from a metal-$5d_z^2$ orbitals based MO to metal-$6p_z$ orbitals based MO in tetranuclear core.

In order to determine the binding mode of the blue complex to ct-DNA, electronic absorption spectroscopy is employed and hyperchromism about 17.5 % is observed, which indicates a weak binding of the blue complex to DNA, such as electrostatic interaction of metal ions or H-bonding through the hydroxyl group of the complex. Voltammetric titration carried out in solution suggested the preferential stabilization of Pt(III) to Pt(II) on binding to DNA. The blue complex inhibits the GSTs activity between 45-200 μM, in sheep liver GST enzyme. The GST enzymes causes drug resistance, therefore inhibition of this enzyme suggests that this complex can be used in combined chemotherapy.

Keywords: Platinum Blues, Mixed-Valenced Platinum Complexes, Sulfur Donor Ligand, Spectroelectrochemistry.

ÖZ

2-AMİNOTİYOFENOL LİGANDININ
PLATİN İLE KOMPLEKSİ: SÜLFÜRLÜ LİGAND İÇEREN
YENİ PLATİN MAVİSİ

Erilhan, İsmail

Yüksek Lisans, Kimya Bölümü
Tez Yöneticisi: Prof. Dr. Hüseyin İşçi
Ortak Tez Yöneticisi: Doç. Dr. Şeniz Özalp Yaman

Haziran 2007, 68 sayfa

K_2PtCl_4 ile 2-aminotiyofenol (H2-atp), $C_6H_5(SH)(NH_2)$, ligandının reaksiyonu sonucunda lacivert katı bir ürün elde edilmiştir. Bu çalışma, bu lacivert katının karakterizasyonu, DNA bağlanma etkileşimi ve enzim aktivitesinin araştırılması ile ilgilidir.

Katı lacivert ürün veya bu çalışmada adlandırıldığı şekliyle "mavi kompleks", asetonda, asetonitrilde ve DMSO içerisinde çözünür olup mavi bir çözelti vermektedir. Çözelti içerisinde kararlı olup, 724 nm'de çok güçlü bir soğurma bandı vermektedir (Asetonda molar soğurma katsayısı platin başına 57782 $M^{-1}cm^{-1}$'dir).

Ürün paramanyetiktir ve XPS'te tek çeşit platin vermektedir (Platin $4f_{7/2}$ ve $4f_{5/2}$ bağlanma enerjileri 71.1 ve 74.6 eV'tur). Element analizi (C, H, N, S, Pt) platinin liganda (2-aminotiyofenolat) mol oranının 1:2 olduğunu göstermiştir. Element analizi, ESR, XPS, ^{1}H-, ^{13}C-, ^{195}Pt-NMR, CV'den elde edilen bilgilerin yorumlanması, bu çalışmada üretilen mavi kompleksin, $[Pt^{III}Pt_3^{II}(2\text{-atp})_8(OH)(H_2O)]$ şeklinde formüle edilebilen yeni bir "platin mavisi" olduğu sonucunu göstermektedir. Bu ürün, köprü ligandının azot ve kükürtten bağlandığı ilk platin mavisi örneğidir. Önerilen molekül yapısı C_{2h} simetrisine sahip $[Pt_2^{II}(2\text{-atp})_4]$ binükleer kompleksinin dimeri şeklinde düşünülebilir. 724 nm'deki bant, metal-$5d_z^2$ orbitallerinden, metal-$6p_z$ orbitallerine serbest bir elektron geçişinden kaynaklanmaktadır.

Kompleksin ct-DNA ile bağlanıp bağlanmadığına karar vermek için elektron soğurma spektrumu kullanılmıştır. % 17.5 dolaylarında hiperkromizm gözlenmesi kompleksin DNA'ya zayıf bir bağla, kompleksteki hidroksil grubundan hidrojen bağıyla veya metal iyonları arasındaki elektrostatik etkileşimle, bağlandığını göstermiştir. Voltametrik titrasyon, DNA bağlanmasında Pt(III)'ün Pt(II)'ye göre daha kararlı olduğunu göstermiştir. Mavi kompleks, 45-200 μM aralığında koyun karaciğerindeki GST enziminin aktivitesini düşürmüştür. GST enzimi ilaç direncine sebep olduğundan, mavi kompleksin bu enzimi inhibe etmesi mavi kompleksin kombine kemoterapide kullanılabileceğini göstermiştir.

Anahtar Kelimeler: Platin Mavisi, Karışık Değerlikli Platin Kompleksleri, Sülfürden Bağlanan Ligandlar, Spektroelektrokimya.

To My Parents

ACKNOWLEDGMENTS

First, I would like to express my sincere thanks to Prof. Dr. Hüseyin İşçi and Assoc. Prof. Dr. Şeniz Özalp Yaman for their supervision, support and encouragement throughout this thesis study.

I would also like to express my special thanks to Prof. Dr. Ahmet M. Önal, Assist. Prof. Dr. Belgin S. İşgör, Assist. Prof. Dr. Atilla Cihaner and Inst. Seha Tirkeş for their help and support.

I am grateful to my family for their support, trust and encouragement.

I would also like to express my thanks to all stuff in METU Chemistry Department and Atılım University Chemistry Group for their support during this study.

TABLE OF CONTENTS

LIST OF TABLES

TABLE

LIST OF FIGURES

FIGURE

CHAPTER 1

INTRODUCTION

1.1. Platinum

Although in use as a metal since at least the 7th century B.C., the chemistry of platinum and the systematic study of its metallurgical and physico–chemical properties did not start until about 250 years ago, following the rediscovery of "platina" (spanish: little silver) in Columbia by the Spanish, and its subsequent announcement in Europe. Platina was by no means a single metal as we know today, but rather an ore that contained approximately ten other metallic elements, among others all the other platinum group metals and Fe, Mn and traces of Cu. It immediately caught the attention of chemists at that time with studies carried out mainly in Spain and England [1].

The 19th century brought the discovery of the first organometallic compound of any metal, $K[PtCl_3(C_2H_4)].H_2O$ by Zeise (1830), and numerous reports on inorganic platinum ammine complexes by scientists such as Peyrone, Reiset, Cossa, Cleve, and Magnus [1]. It was the 'Theory of Coordination' of Werner, which by the end of 19th century, provided an explanation for the constitution of many of these complexes. During the 20th century the development of metal catalysts for industrial production processes, many of which contain Pt or platinum group metals [2], was a major goal. Termed once a "master of transmutation", platinum has been estimated to be used in the manufacture of one out of five of today's products [3].

Rosenberg's serendipitous discovery of the ability of a metal coordination compound, *cis*-$Pt(NH_3)_2Cl_2$, to block DNA replication and cell division [4] and subsequent findings that the very same agent, then termed "*cisplatin*", and many structural analogues are potent antitumor agents [5], has influenced tremendously the

development of inorganic metal coordination chemistry over the last 30 years. For the first time the usefulness of drugs containing a heavy metal in cancer chemotherapy had been demonstrated. Today *cisplatin* is considered one of the most successful antitumor agents [6]. It is generally agreed upon that the discovery of *cisplatin* and attempts to understand its mode of action had a substantial impact on the research of interactions between metal ions and living matter in general, and on the whole field of bioinorganic chemistry [7].

1.2. Platinum Blues

A family of deeply colored platinum compounds, usually called platinum blues, has attracted wide interest for years not only because of their unusual color and intriguing chemistry, but also for their high antitumor activities [8]. In contrast to the usual yellow, orange, red, or colorless platinum complexes, platinum blues are unusual for their intense blue or purple colors [9]. The first blue platinum compound was prepared by German chemists in 1908 [10]. This unusual material was prepared by the reaction of Ag_2SO_4 with yellow cis- $Pt^{II}Cl_2(CH_3CN)_2$ and was first proposed to have a mononuclear composition of $Pt^{II}(CH_3CONH)_2.H_2O$. However, the compound was later proposed to be polymeric with bridging acetamidate linkages [11]. Owing to later studies made by using cis-$Pt(NH_3)_2Cl_2$, it is thought that the original "platinblau" may have the structural framework illustrated in Figure 1 or one having slightly modified bridging modes [9].

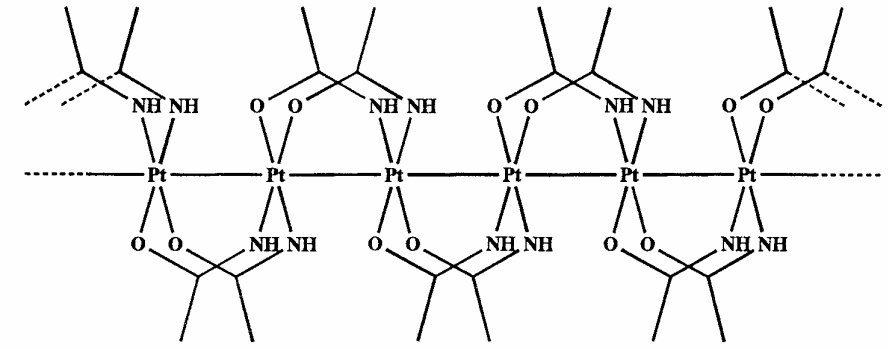

Figure 1. A possible polymeric structure of the original blue $Pt(CH_3CONH)_2$.

In order to account for the origin of the blue color, various platinum blues compounds were further prepared with a variety of amide ligands, mostly using K_2PtCl_4 as the starting material [12-22]. However, none of these studies afforded a clear conclusion about the structure and the formula, due to the failure of obtaining single crystals suitable for determining the structure using X-rays.

Several decades later, progress was made in determining the chemistry of platinum blues by employing the "cis-$Pt(NH_3)_2$" moiety of cis-$Pt(NH_3)_2Cl_2$. Since Rosenberg discovered the antitumor activity of cis-$Pt(NH_3)_2Cl_2$ (cis-DDP, *cisplatin*) [23-26], the chemistry of cis-DDP and its analogs have received considerable attention because of their potential application as anticancer drugs. Moreover, special attention was paid to the platinum blues produced from the reactions between the hydrolysis product of cis-DDP (i.e., cis-$[Pt(NH_3)_2(OH_2)_2]^{2+}$) and pyrimidine bases such as uracil, since these so-called "platinum-pyrimidine-blues" were found to have a high index of antitumor activity with a lower associated nephrotoxicity than cis-DDP [27-28]. The medical interest thus required chemists to unveil the structure of platinum blues. However, no structural evidence for the platinum-pyrimidine-blues was obtained until the first structural analysis of α-pyridonate-blue was reported [29-30].

The first direct evidence for the structure of platinum blues was provided by the single-crystal X-ray studies of cis-diammineplatinum α-pyridonate-blue, $[Pt(2.25+)_4(NH_3)_8(\mu\text{-}\alpha\text{-pyridonato-N,O})_4](NO_3)_5 . H_2O$ [29-30]. Figure 2 shows an ORTEP view of the α-pyridonate-blue cation. The chemical formula and the structure reveal that the complex cation is mixed-valent, comprised of three Pt(II) and a Pt(III) atoms, whose platinum oxidation state is formally expressed as $Pt^{II}{}_3Pt^{III}$ (abbreviated as $Pt(2.25+)_4$), and the tetraplatinum chain structure is composed of two binuclear cis-$[Pt_2(NH_3)_4(C_5H_6NO)_2]^{n+}$ units, having two amidate bridging ligands in a head-to-head arrangement. One Pt(III) atom has one unpaired electron and imparts paramagnetism to the compound. Both the intra- and interdimer Pt-Pt distances 2.7745 and 2.8770 Å, respectively, revealed that the platinum centers are metal-metal bonded to each other [29].

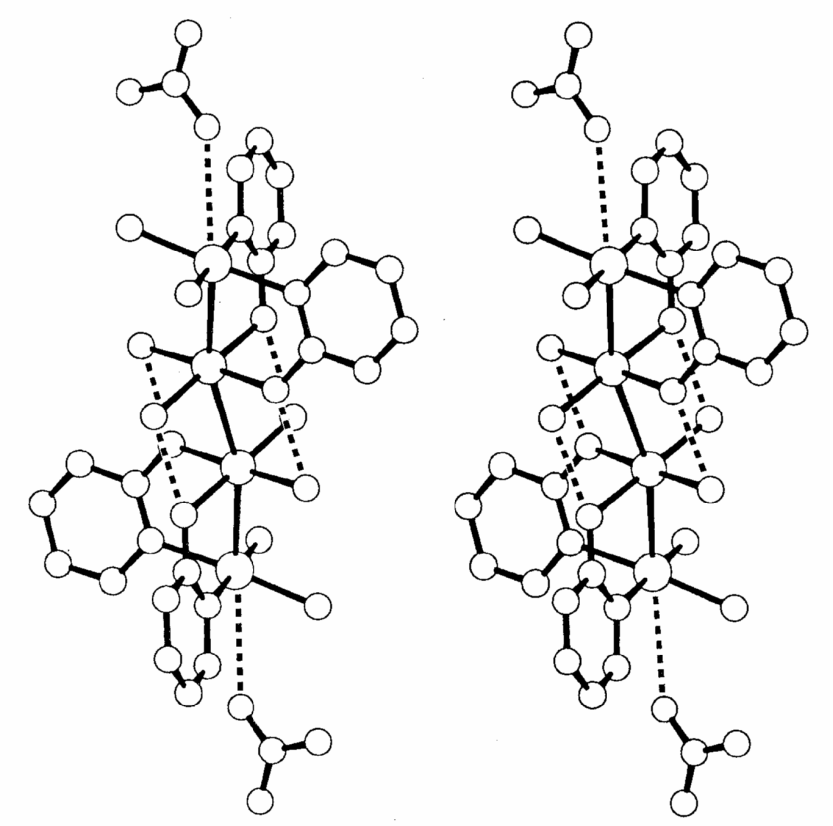

Figure 2. Stereodiagram for the $[Pt(2.25+)_4(NH_3)_8(\mu\text{-}\alpha\text{-pyridonato})_4]^{5+}$ cation, together with the loosely associated nitrate ions.

Following these reports, several structural analogues with different average platinum oxidation states, Pt(2.0+), Pt(2.25+), and Pt(2.5+), and Pt (3.0+) have been structurally characterized. These oxidation states correspond to their formal oxidation states of $Pt(II)_2$, $Pt(II)_3$ $Pt(III)$, $Pt(II)_2Pt(III)_2$, and $Pt(III)_2$, respectively [9].

In addition to this classification, the structures can also be grouped according to the orientation of the two bridging amidate ligands within a dimeric unit; head-to-head (HH) and head-to-tail (HT) are known to $Pt(II)_2$ and $Pt(III)_2$ compounds [31-32-33-34]. However, only the HH isomers afford a dimer of dimers, leading to the tetraplatinum chain structure of platinum-blues. On the other hand, the HT isomers do not dimerize to give the tetramer due to the steric bulk of the exocyclic amidate

rings at the ends of the dimeric unit. But this is not the case for amidate-bridged dimer compounds with chain (or acyclic) amidates such as acetamidate. The third classification is related to the nuclearity of the complex; two major groups exist, dimer and tetramer. In addition, the chain structures are classified based on whether they have axial ligands. All these classified structures are shown in Figure 3. In addition to these dimeric and tetrameric structures, two other groups, illustrated in Figure 4, are also known. Compounds E1 [35] and E2 are produced as a result of deprotonation at one of the four equatorial ammine ligands of the dinuclear α-pyrrolidonate Pt(3.0+) species. Two octanuclear platinum-blues (F1) are known when acyclic amidate (acetamidate and 2-fluoroacetamidate) is employed instead of cyclic ones [36-38].

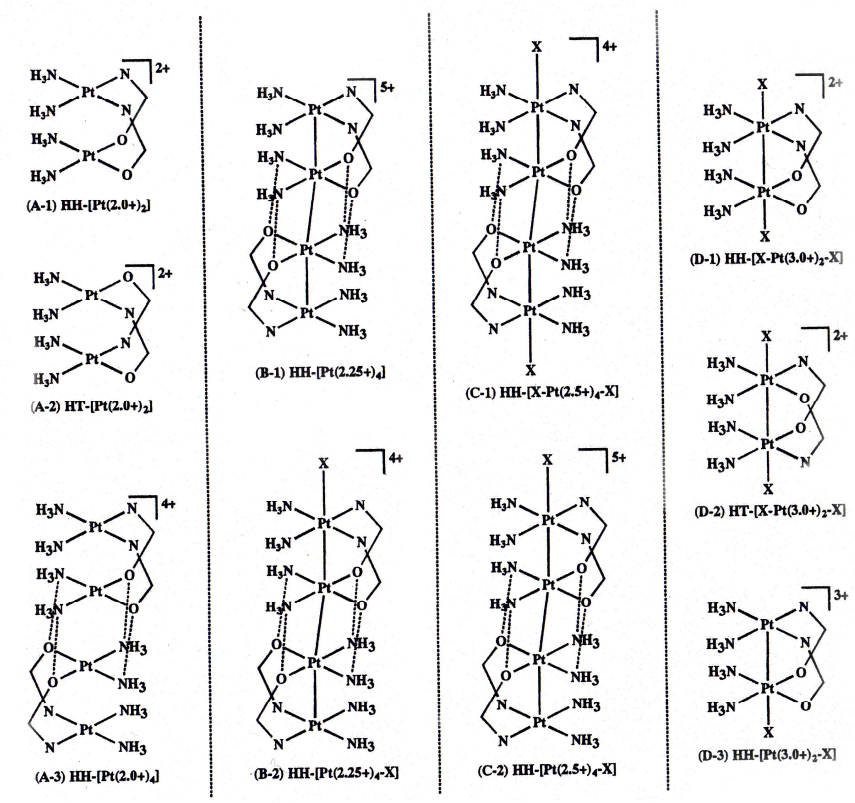

Figure 3. Different structures identified by X-ray diffraction, where the abbreviated N-O is used to express each bridging amidate ligand and X denotes axial donors such as OH_2, NO_3^-, NO_2^-, Cl^-, and Br^-.

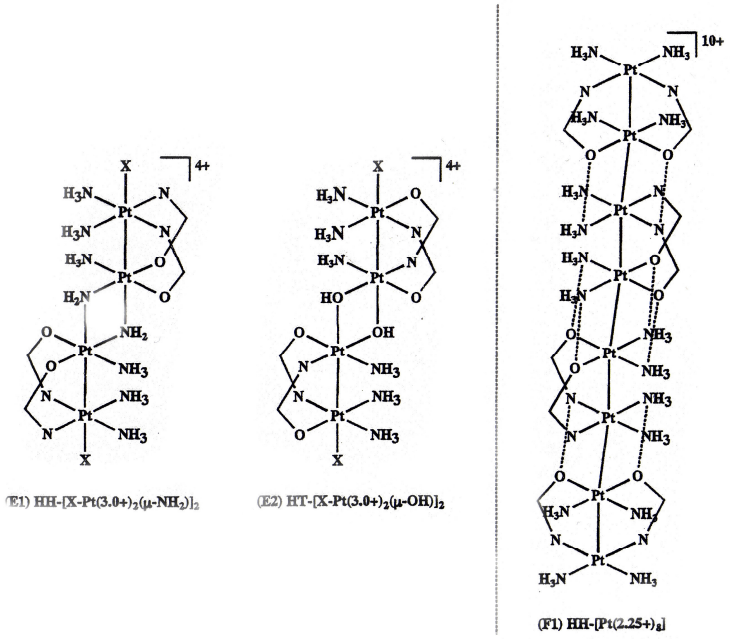

Figure 4. Two novel structures observed for $Pt(3.0+)_2$, and an octaplatinum chain structure observed in the acyclic amidate systems.

1.3. Antitumor Active Platinum-Blues

Cisplatin was chemically described in 1845, but its antitumor properties were only found accidentally by Rosenberg in 1965. While investigating the influence of an electric field on the growth of the E.coli bacteria, Rosenberg found that cells stopped dividing and displayed strong filamentous growth. Following this discovery a large number of platinum complexes were tested for their antiproliferative effect. The complexes having cis geometry were found to be antitumor active and *cisplatin* is the most active one. The trans isomer of $Pt(NH_3)_2Cl_2$, *transplatin*, showed no antitumor activity. The structures of *cisplatin* and *transplatin* are shown in Figure 5.

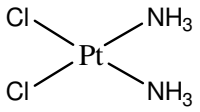

Cisplatin

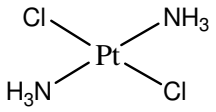

Transplatin

Figure 5. Structure of the antitumor drug, *cisplatin*, and its inactive trans isomer, *transplatin*.

Cisplatin successfully entered into clinical trials in 1971. The first clinical test was performed by Hill et al. and was approved by the United States FDA in 1978. *Cisplatin* is routinely used in the clinic, appearing the most effective against testicular and ovarian cancer. With testicular cancer, when recognized in an early stage, curing rates exceed 90%.

Common problems associated with *cisplatin* in the clinic include nephrotoxicity, mototoxicity and myelosuppression. Toxic side effects of *cisplatin* limit the dose that can be administrated to patients.

The other main reason for a failure of *cisplatin* chemotherapy is resistance of tumors to the drug. The resistance can be intrinsic or acquired and limits the applicability of *cisplatin* to a relatively narrow range of tumors.

The most significant advantage in obviating the side effects of *cisplatin* has become from the process of analogues development, i.e. the search for structural analogous *cisplatin* that fulfill one or all of the next criterions:

1. Development of new selectivities, including an activity spectrum wider than *cisplatin* and, especially, activity in *cisplatin*-resistant tumors.
2. Modification of the therapeutic index, that is to say, a higher clinical efficacy to reduce toxicity, with activity at least in the same range as *cisplatin*.
3. Modification of the pharmacological properties, such as solubility, which could result in improved ways of administration.

New antitumor drugs are designed to increase therapeutic efficacy. Efforts have been made to found compounds that are more effective and have an acceptable effect on the patient's quality of life. Thus,

1. to develop orally active platinum drugs,
2. to reduce serious side effects,
3. to overcome drug resistance

are the main goals of producing new drugs.

Since the discovery of antitumor activity of *cisplatin*, a large number of new compounds have been synthesized and tested for antitumor activity.

1.4. The Present Work

One of our research interests is to investigate binuclear metal complexes, in particular, platinum ones [46,125]. The general formula of these complexes can be represented as $[M_2(B\text{-}B)_4]^{n-}$ or $[M_2(B\text{-}B)_4X_2]^{n-}$, where, M = Cr, Mo, W, Te, Re, Ru, Os, Rh, Pt; B-B = homo- or hetero-donor bidentate bridging ligand, such as RCO_2^-, CO_3^{2-}, SO_4^{2-}, HPO_4^{2-} (oxygen donors); $H_2P_2O_5^{2-}$ (phosphorus donor); RCS_2^- (sulfur donor); $RCONH^-$, α-pyridonate (oxygen and nitrogen donor); pyrimidine-2-thionate (sulfur and nitrogen donor); X = axial monodentate ligand. They all have a common structure, which consists of two square-planar MO_4, MP_4, MS_4, MO_2N_2, MN_2S_2 units linked together face to face given usually an eclipsed or almost eclipsed M_2O_8, M_2P_8, M_2S_8, $M_2N_4O_4$, $M_2S_4N_4$ (nitrogen-oxygen, nitrogen-sulfur donors) cluster with short metal-metal distances (Figure 6). Monodentate ligands occupy axial positions. These compounds are also important from the cluster chemistry stand point, because they represent the simplest metal clusters.

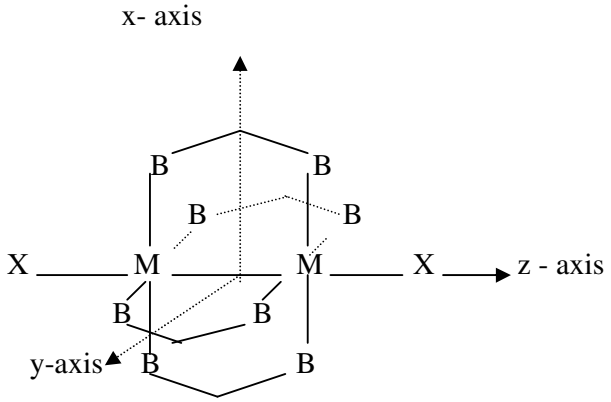

Figure 6. The structure of a binuclear complex with the general formula $[XM(B\text{-}B)_4MX]^{n-}$.

The easiest way to visualize metal-metal bonding is to consider the overlap of d-orbitals on each metal atom in a binuclear metal cluster, M_2 (Figure 7). If we assume metal-metal axis is the z-axis of our coordinate system, $d_{x^2-y^2}$ will be used in metal-ligand bonding, so metal-metal bond will result from the overlap of four d-orbitals on each metal atom. These are $d_{z^2}(\sigma)$, $d_{xz}(\pi)$, $d_{yz}(\pi)$ and $d_{xy}(\delta)$. Thus we will have 4 bonding molecular orbitals (one σ, two π and one δ), and four antibonding molecular orbitals.

The metal-metal bond order of these complexes changes from four to zero according to the number of electrons filling these orbitals. The highest bond order is for d^4-d^4 system, which is four and the lowest bond order is for d^8-d^8 system, which is zero. In general there is a relationship between calculated bond order and the observed metal-metal distance. As the bond order increases the metal-metal distance decreases.

As part of our effort to further our understanding the chemistry of binuclear complexes, we tried to prepare a new binuclear platinum complex by reacting K_2PtCl_4 with 2-aminothiophenol (H2-atp) in basic aqueous solution (Figure 8). When appropriate experimental conditions were employed a dark blue solid product was obtained. This blue product, which will be referred as “the blue complex” in this thesis, is a new mixed-valance platinum blues with sulfur and nitrogen donors

bridging bidentate ligand, 2-aminothiophenolate (2-atp) anion. The blue complex has a very intense absorption band, at 724 nm, in its absorption spectrum in acetonitrile.

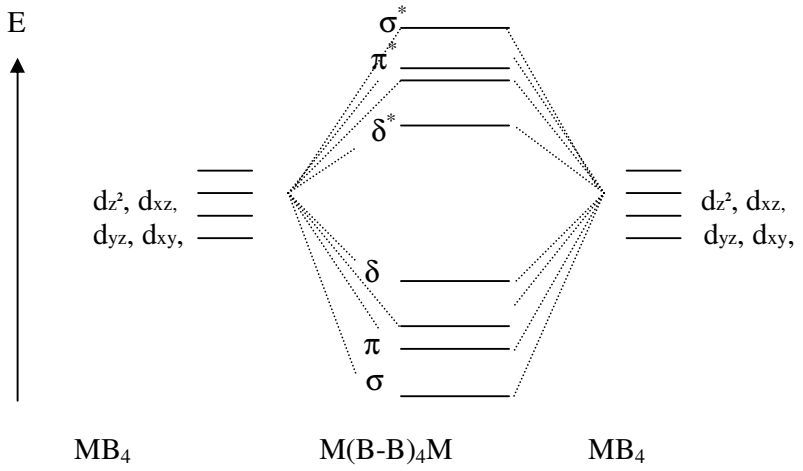

Figure 7. The relative energies and symmetries of the molecular orbitals resulting from metal-metal bonding in $M(B\text{-}B)_4M$ complex.

In the first part of this work we tried to characterize the nature of the blue complex by using UV-Vis, ESR, XPS, SEM, ^{1}H-, ^{13}C- and ^{195}Pt-NMR, cyclic voltammetry, elemental analysis techniques. In the second part, preliminary DNA binding studies and enzymatic activity studies of the blue complex are performed.

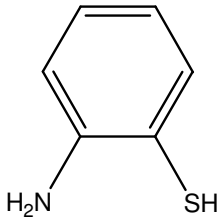

Figure 8. Molecular structure of 2-aminothiophenol (H2-atp).

CHAPTER 2

EXPERIMENTAL PART

2.1. Preparation of Compounds

The starting material for the platinum complexes was metallic platinum. The ligand, 2-aminothiophenol, is obtained commercially (ACROSS).

2.1.1. Preparation of $H_2[PtCl_4]$

7.70 g of platinum metal was cut into very small pieces and dissolved in 70 mL aqua regia. The mixture is evaporated until the volume decreased to 20 mL, and 50 mL of concentrated HCl is added in order to complete the volume back to 70 mL. This process is repeated for six times. Finally 30 mL of orange colored H_2PtCl_6 solution is obtained. Stoichiometric amount of hydrazine dihydrogendichloride $N_2H_4.2HCl$ is dissolved in 30 mL water and added to H_2PtCl_6 solution drop by drop to reduce Pt(IV) to Pt(II). Resulting cherry red solution is cooled in the refrigerator overnight. The solution might have contained small amount of H_2PtCl_6. Therefore, in order to precipitate $[PtCl_6]^{2-}$ as $(NH_4)_2[PtCl_6]$, saturated ammonium chloride solution is added to cherry red solution drop by drop while stirring. Orange colored $(NH_4)_2[PtCl_6]$ precipitates are separated by filtration. This procedure is repeated until no more precipitation occurred. The amount of platinum in the cherry red solution is determined by ash analysis as 0.1007 g/mL, which is used as stock solution (H_2PtCl_4) for further preparations.

2.1.2. Preparation of $K_2[PtCl_4]$

15 mL from the stock solution of H_2PtCl_4 (0.1007 gPt/1mL) is taken and reacted with stoichiometric amount of saturated aqueous solution of potassium chloride. The mixture is evaporated to dryness and at the end red crystals of $K_2[PtCl_4]$ is obtained. The percent yield was 85.13 %.

$$H_2PtCl_4(aq) + 2\ KCl(aq) \rightarrow K_2[PtCl_4](aq) + 2\ HCl(aq) \qquad (1)$$

2.1.3. Preparation of the Blue Complex

100.2 mg (0.241 mmol) of K_2PtCl_4 was dissolved in 5 mL of deionized water in 20 mL round bottom flask and pH of the solution was adjusted to 13 using concentrated aqueous solution of NaOH. Then, 2 mL DMF solution of 57.48 µL H2-atp (0.48 mmol) ligand was added to the K_2PtCl_4 solution drop wise while stirring. An immediate yellow precipitate formation was observed. The solution at this stage was acidic. A few drops of sodium hydroxide solution was added to this mixture until the pH was about seven and then refluxed in an oil bath at 40ºC for about 2 hours. In the first quarter of reflux, the color of the solution was changed from yellow to dark green. At the end of reflux, the color turned to navy blue. The solution was removed from the oil bath and cooled down first at room temperature and then in refrigerator for 2 hours. The dark blue solid was collected by suction filtration using a sintered glass funnel, washed with water and dried under vacuum at room temperature. The yield was 82.50 mg.

$$PtCl_4^- + 2\ (H2\text{-}atp) \xrightarrow[pH = 13]{RT} Pt^{II}(2\text{-}atp)_2 + 2HCl\ \text{(yellow product)} \qquad (2)$$

$$2\ Pt^{II}(2\text{-}atp)_2 + 2H_2O \xrightarrow[pH =7,\ 30\ min]{40^o\ C} Pt_2^{II,II}\ (2\text{-}atp)_4.2H_2O\ \text{(green product)} \qquad (3)$$

40^o C

$$2\ Pt_2^{II,II}(2\text{-atp})_4.2H_2O \xrightarrow[pH=7,\ 2\ h]{} Pt(2.25+)_4(2\text{-atp})_8(OH)(H_2O) + H^+ + 2\ H_2O \quad (4)$$

Elemental Analysis:

Anal. Calc. For $Pt_2S_4N_4H_{28}C_{24}O_2$ (green product):

C: 31.2%, H: 3.06%, N: 6.07%, S: 13.9%; Found: C: 29.9%, H: 2.61%, N: 5.87%, S: 13.6%. Volhard method indicated no chlorine presence.

Anal. Calc. For $Pt_4S_8N_8H_{51}C_{48}O_2$ (blue product):

C: 31.9%, H: 2.84%, N: 6.19%, S: 14.2%; Found: C: 32.5%, H: 2.87%, N: 6.83%, S: 14.8%. Volhard method indicated no chlorine presence.

Anal. Calc. For $Pt_4S_8N_8H_{50}C_{48}O$ (blue product):

C: 32.2%, H: 2.76%, N: 6.26%, S: 14.3%; Found: C: 32.5%, H: 2.87%, N: 6.83%, S: 14.8%.

Pt-Ash Analysis calculated for $Pt_4S_8N_8H_{51}C_{48}O_2$: Pt: 43.14%, Found: Pt: 42.07%.

SEM Analysis (blue product): Presence of platinum, nitrogen and sulfur atoms is detected. There is no chlorine atom.

2.2. Electrochemistry

2.2.1. Cyclic Voltammetry

Cyclic voltammetry (CV) is known as a potential-controlled electrochemical experiment, which yields information on the I-E (current-potential) dependence. During CV measurements, a cyclic potential sweep is applied on an electrode resulting a current response. A potentiostat system controls the parameter, imposes on an electrode a cyclic linear potential sweep and outputs the resulting current-potential curve.

The electrochemical reaction under study takes place at the working electrode (WE). The electrical current at the working electrode is called faradaic current. Solid disk electrodes are the most common WE used in CV experiments. Platinum, glassy carbon, gold, and silver are also used. An auxiliary or 'counter' electrode (CE) is used to balance the faradaic process at the WE having an electron transfer of opposite direction. A reference electrode (RE) is also needed and the most common ones are Ag/AgCl and the calomel electrode. The CV response is plotted as current versus potential. During the forward sweep the reduced form is oxidized and on the reverse sweep the oxidized form near the electrode is reduced again. In the case of having a chemical reaction, the shape of the CV is affected. The absence of the reversed peak means that the oxidized species have been removed by a chemical reaction.

Electrochemical behavior of our complex and H2-atp was investigated by cyclic voltammetry using Volta Lab PGZ 301 Dynamic Voltammetry. The cell, which is used for the cyclic voltammetry analysis is presented in Figure 9.

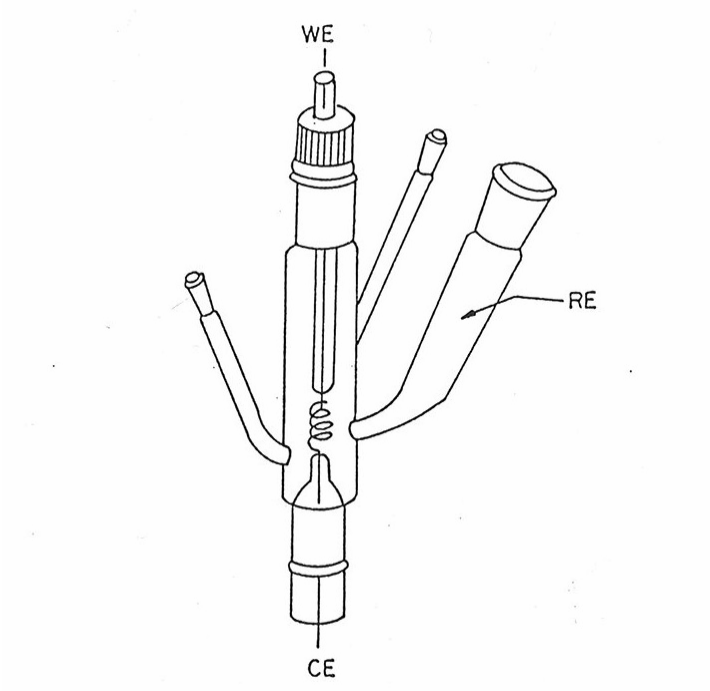

Figure 9. The cyclic voltammetry cell; WE: Pt-bead, CE: Pt-wire, RE: Ag-wire or SCE.

Cyclic voltammetry studies were made in acetone-$[(n\text{-}C_4H_9)_4N]BF_4$ (tetra-n-butylammoniumtetrafluoroborate) solvent electrolyte couple at room temperature. Argon gas was allowed to pass through the solution prior to each measurement in order to eliminate oxygen from the system.

A three-electrode system was used during cyclic voltammetry studies. In this system, Ag-wire or SCE (saturated calomel electrode) were used as reference electrode, platinum bead or glassy carbon electrodes were used as working electrode and platinum wire or coil electrodes were used as auxiliary (counter) electrode. Those three electrodes were positioned as close as possible in order to minimize IR drop.

The concentration of our complex and H2-atp was about 0.001 M for each measurement. Scan rate during the recording of cyclic voltammograms was 100 mV/s or 200 mV/s.

2.2.2. Spectroelectrochemistry

Constant potential electrolysis of ligand H2-atp, and the blue complex at their peak potentials were carried out in acetone-$[(n\text{-}C_4H_9)_4N]BF_4$ solvent-electrolyte couple versus Ag-wire reference electrode. Platinum gauze (0.5 cm^2) electrodes served as working and counter electrode as well. The electrolysis cell, which was used for the in *situ* measurements at room or below temperatures, is given in Figure 10.

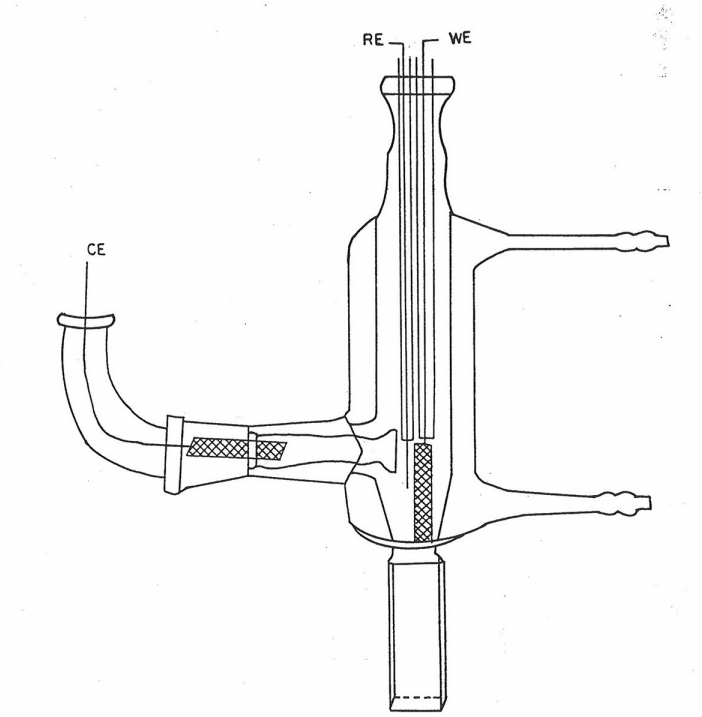

Figure 10. The electrolysis cell used for in *situ* measurements of UV-Vis spectrum of the electrolysis solution; WE: Pt gauze, CE: Pt-plate, RE: Ag-wire.

Electronic absorption spectra were recorded for every 50 mC intervals in *situ*, using HP 82524A Diode Array Spectrophotometer. During the electrolysis, nitrogen gas was purged through the electrolysis solution for stirring purposes between the scans.

2.2.3. Coulometry

Coulometric analyses were made by chronocoulometric method, in which quantity of charge versus time is recorded. The total quantity of charge, which is obtained from the point corresponding to the plateau of the curve, is used to calculate the number of electrons.

Chronocoulometry of the ligand and the complex were carried out at the peak potentials in acetone-$[(n\text{-}C_4H_9)_4N]BF_4$, solvent-electrolyte system using Volta Lab PGZ 301 Dynamic Voltammetry at platinum gauze electrodes versus Ag-wire.

2.3. Electron Spin Resonance

ESR (or EPR) spectra of blue complex in the solid powder form and in frozen acetone were recorded by using Bruker Xepr Elexsys-580 Spectrometer in quartz ESR-cell at various temperatures (from + 25°C to -150°C), where diphenyl picryldihydrazyl (DPPH) was used as a reference.

2.4. Nuclear Magnetic Resonance

^{1}H-, ^{13}C- and ^{195}Pt-NMR spectra of ligand and blue complex were recorded on Bruker GmbH DPX-400, 400 MHz High-Performance Digital FT NMR, using acetone-d_6 as a solvent and TMS as an internal reference.

2.5. Scanning Electron Microscope (SEM)

Analysis of the surface morphologies of blue complex were done by using JEOL JSM-6400 scanning electron microscope.

2.6. X-Ray Photoelectron Spectroscopy (XPS)

XPS spectrum of blue complex was measured by using SPECS ESCA system with Mg/Al dual anode.

2.7. DNA Binding Studies

2.7.1. Preparation of Tris Buffer Solution

5 mM (80.1 mg) Tris.HCl ($C_4H_{11}NO_3$.HCl) and 50 mM (292.7 mg) NaCl were placed in a 100 mL flask and dissolved in approximately 70 mL deionized water. pH of the solution was adjusted to 7.0 with 1.0 M NaOH before making the volume 100 mL.

2.7.2. UV Titration

UV titration of the platinum blue complex was performed in tris buffer-acetone mixture (2:10) for R=0, 2, 4, 6, 8 and 10, where R is the concentration ratio of ct-DNA(calf thymus) to the platinum blue complex. Prior to each measurement ct-DNA and platinum blue complex were incubated about 15 minutes. The changes in the electronic absorption spectrum were recorded by using HP 82524A diode array UV-VIS spectrophotometer.

2.7.3. Voltammetric Titration

Voltammetric titration of platinum blue complex with ct-DNA was carried out by using cyclic voltammetry in tris buffer, which contains 20% acetone. The voltammetric changes were recorded for R= 0, 5 and 10 (R= [DNA]/[Pt-complex]) by using Volta Lab PGZ 301 Dynamic Voltammetry. Ag-wire was used as a reference electrode. Glassy carbon electrode and Pt-wire electrode were employed as a working and auxiliary (counter) electrode, respectively. Measurements were made under argon gas atmosphere.

2.7.4. Enzymatic Activity

1-chloro-2,4-dinitrobenzene (CDNB), reduced glutathione (GSH), were purchased from Sigma Chemical Company, St. Louis, MO, U.S.A. Cytosols of sheep liver were supplied from METU (Group of Assoc. Prof. Dr. Nursen Çoruh in Chemistry Department).

2.7.5. Determination of Cytosolic GSTs Activity

The GST (Glutathione S-Transferase) activity is determined against the substrate 1-chlor-2,4-dinitrobenzene (CDNB). The enzyme activity assay was conducted at room temperature. GST activity against the CDNB was determined spectrophotometrically by monitoring the formation of the conjugation product under the condition given in Table 1 and 2 [39-41]

Table 1. Composition of the reaction mixture for GSTs activity measurements against CDNB.

Constituents of The Reaction Mixture	**Added volume (µl)**
Substrate Solution	50
Combination Solution - Buffer - 50.0 mM GSH, - H_2O,	900
Enzyme Source - Sheep Liver Cytosol	50

Table 2. Composition of the reaction mixture for total GST activity measurements against CDNB in the presence of the blue complex.

Constituents of The Reaction Mixture	**Added volume (µl)**
Substrate Solution	50
Combination Solution - Buffer - 50.0 mM GSH, - H_2O,	800
Drug (The Blue Complex)	100
Enzyme Source - Sheep Liver Cytosol	50

CHAPTER 3

RESULTS AND DISCUSSION

3.1. Synthesis and Identification of the Blue Complex, a Novel Platinum Blues

Binuclear metal complexes of general formula $[M_2(B\text{-}B)_4X_2]^{n-}$ where B-B is bridging bidentate ligand with homo or hetero donor atoms and X is a monodentate ligand which is relatively weakly coordinated to the metals at axial positions, have a lantern structure (Figure 6), with relatively short metal-metal distance [42]. They have attracted increasing attention in the last three decades due to their potential use as drugs for cancer therapy [43], catalysts for industrially important reactions [44], and precursors for the preparation of materials with unusual physical properties [45]. They have emerged as a new class of metal complexes to be explored.

For the last twenty years we have been interested in studying the properties of binuclear metal complexes. Thus in our research lab we investigated the electronic, structural, axial ligand substitution reaction kinetics, electrochemical and chemical redox properties of some binuclear metal complexes [46,125].

As continuation of this research, in this thesis work, we aimed to synthesize new binuclear complexes. The potential bridging ligands chosen were 2-aminothiophenol, 3-aminothiophenol and 4-aminothiophenol, and the metal was platinum. No work has been reported in the literature on the complexes of platinum with aminothiophenol ligands. Among the three ligands, 4-aminothiophenol is unstable at room temperature, and in 3-aminothiophenol the donor atoms were too far apart to bridge the two platinum atoms in binuclear complex structure.

The reaction of 2-aminothiophenol (H2-atp), with K_2PtCl_4 in water yielded yellow precipitate (Figure 11). The yellow precipitate was insoluble in common solvents, such as water, acetonitrile, acetone, dichloromethane, ethanol, DMF and DMSO, therefore we were not able to measure the electronic absorption spectrum of it. Stoichometric experiments made in the synthesis have suggested that the metal to ligand ratio is 1:2. The complex is most likely to be a monomeric square-planar complex of platinum(II), as $[Pt(2\text{-}atp)_2]$.

$$K_2PtCl_4\ (aq) + 2\ H2\text{-}atp\ (l) \longrightarrow [Pt(2\text{-}atp)_2]\ (s) + 2KCl\ (aq) + 2HCl\ (aq) \quad (5)$$

(yellow product)

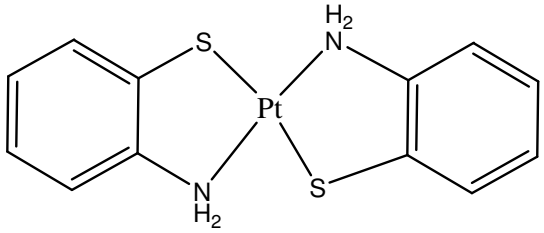

Figure 11. The proposed molecular structure of the yellow product.

The same reaction was carried out at a little higher temperature, 40ºC, in order to increase the yield of the yellow product. In the course of the reaction, the yellow product was precipitated first, but then the color of precipitate changed to green when heated to 40ºC for about 30 minutes while stirring. Green product was collected and analyzed by elemental analysis, SEM analysis and chemical methods (volhard method). SEM measurements revealed the presence of Pt, N and S atoms, whereas no chlorine atoms were detected. Volhard method was also used to check the absence of chlorine; the result was consistent with SEM analysis.

The elemental analysis of the green product suggested that the metal to ligand ratio is still 1:2, and it is consistent with the formula as $[Pt_2(2\text{-atp})_4.(H_2O)_2]$.

$$2\ [Pt(2\text{-atp})_2]\ (s) + 2H_2O\ (l) \longrightarrow [Pt_2(2\text{-atp})_4.(H_2O)_2]\ (s) \quad (6)$$
(green product)

The green product was insoluble in any common solvents, thus solution absorption spectrum could not be measured. On the bases of our experimental observation this product is a binuclear complex of platinum (II) with 2-atp bridging ligand (Figure 12).

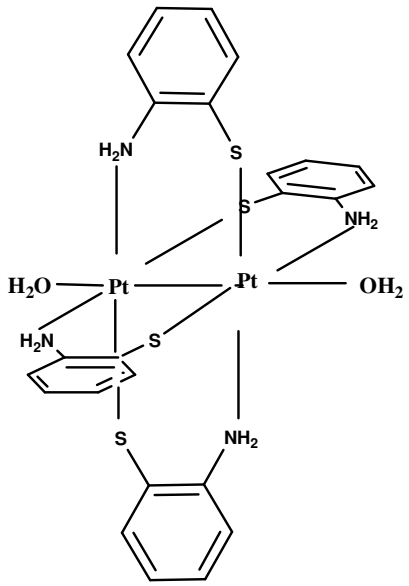

Figure 12. The proposed molecular structure of the green product (H-H isomer).

In one of the trial synthesis experiment a very dark blue colored solid was isolated accidentally. Unlike the yellow and green product, the dark blue solid, which

we call it “the blue complex”, was pretty soluble in acetone and in acetonitrile and yielded blue colored solution. The electronic absorption spectrum of the blue complex in acetonitrile has a very intense band at 724 nm, which is responsible for the dark blue color. This observation was very exciting in the sense that first, 724 nm band might have indicated the presence of very strong metal-metal interaction; second, this might have been a new platinum blues, which constitute a family of complexes generally containing a chain of four platinum atoms of mixed valences and metal-metal bonds. When we wanted to prepare more of this blue product by reacting K_2PtCl_4 with H2-atp we ended up with yellow or green product. It took real effort and a lot of experimentations to develop the procedure to reproducibly synthesize the blue complex, described in the experimental part.

When the green product in water acidified, it was converted to the yellow product. This observation indicated that the pH of the reaction medium is an important factor in determining the product complex. The ligand H2-atp is an amine, therefore it is a base, on the other side it is a thiol, and therefore it can also be considered as an acid. Increasing the pH of the solution increases the coordinating ability of the amine nitrogen, and the thiol sulfur. Upon coordination of H2-atp ligand from the sulfur atom it releases a proton, thus making the reaction mixture acidic. In acidic medium amine nitrogen is protonated. This will decrease the coordination ability of the ligand from the nitrogen atom. Thus, keeping the pH of the reaction medium at about seven or little higher than seven is the crucial point for the synthesis of the blue complex.

The C, N, H, S and Pt analysis of the blue complex indicated that the metal to ligand ratio is 1:2 and the best fit to the found analysis is obtained by assuming the molecular formula as $[Pt_4(2\text{-atp})_8(OH)(H_2O)]$ with an average oxidation state of the platinum is “+2.25”. This can be visualized as three Pt(II) and one Pt(III) in the unit formula (Figure 13).

$$2\ Pt_2(2\text{-atp})_4.(H_2O)_2\ (s) + H_2O\ (l) \longrightarrow [Pt_4(2\text{-atp})_8(OH)(H_2O)]\ (s) \quad (7)$$
(blue complex)

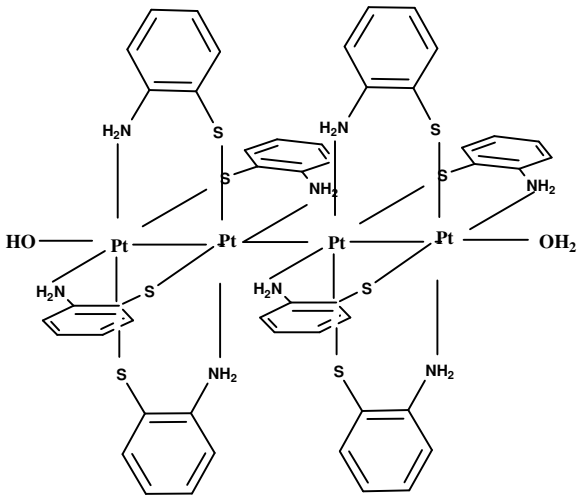

Figure 13. The proposed molecular structure of the blue complex.

As seen from the proposed structure of the blue complex shown in Figure 13, it is a dimer of HH-binuclear complexes, with OH^- and H_2O coordinating to the two end-platinum atoms at axial positions. The most probable structure must allow the hydrogen bonding type interaction between the hydrogens of the amine groups of one binuclear unit with the lone pair electrons on the sulfur of the other binuclear unit. In addition to the metal-metal interactions between the dimers, the above mentioned hydrogen bonding type interaction may be the main driving force for the formation of the blue complex.

3.1.1. The Electronic Absorption Spectra and Molecular Orbital (MO) Energy Levels

The electronic absorption spectra of H2-atp, the ligand, and the blue complex measured in acetonitrile are given in Figure 14 and Figure 15, respectively. Spectral data, indicating band positions and the molar absorptivities are tabulated in Table 3. The electronic absorption spectrum of the blue complex was also measured in acetone. Two segments of the spectrum in acetone, higher energy side (350-600 nm) and lower energy side (800-1000 nm) of the most intense band at 724 nm are shown in Figures 16 and 17, respectively. Spectral data are included in Table 3.

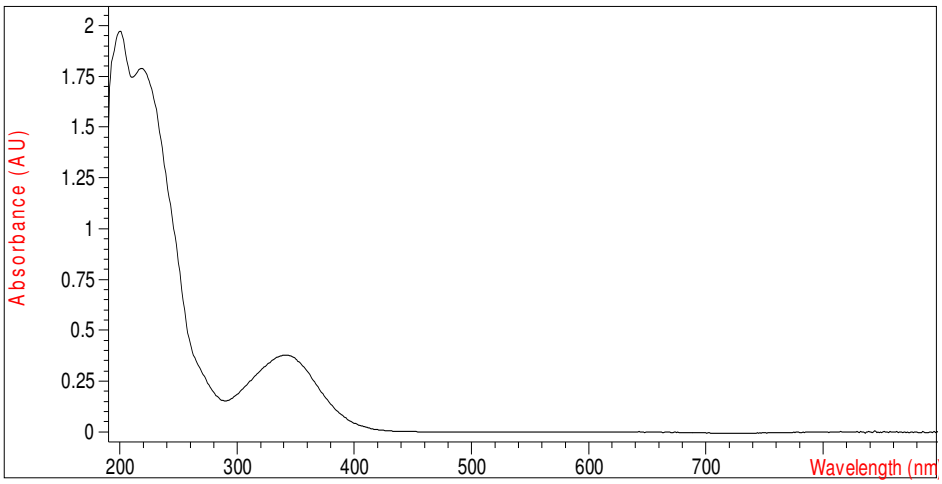

Figure 14. The electronic absorption spectrum of the ligand, H2-atp, in acetonitrile (Concentration of H2-atp = 9.64 x 10^{-4} M).

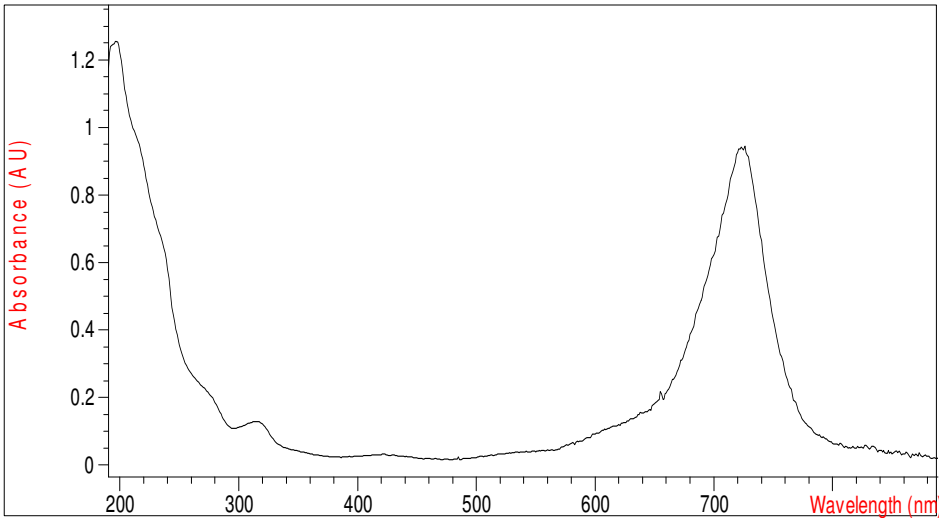

Figure 15. The electronic absorption spectrum of the blue complex in acetonitrile (Concentration based on the formula as $[Pt_2(2\text{-atp})_4(H_2O)(OH)]$ =1.11x10^{-5} M).

Table 3. Electronic absorption spectral data for the blue complex. (Calculated molar absorptivities are based on the molecular formula $[Pt_4(2\text{-}atp)_8(H_2O)(OH)]$ = 1808.81 g/mol and for $[Pt_2(2\text{-}atp)_4(H_2O)(OH)]$ = 921.92 g/mol)

In Acetone			
Band No	**λ(nm)**	**ε($M^{-1}cm^{-1}$)**	
		For $[Pt_4(2\text{-}atp)_8(H_2O)(OH)]$	**For $[Pt_2(2\text{-}atp)_4(H_2O)(OH)]$**
I	418	13275	6773
II	539	10672	5445
III	610	18642	9511
IV	724	226505	115564
V	832	10915	5569
VI	949	7642	3899
In Acetonitrile			
Band No	**λ(nm)**	**ε($M^{-1}cm^{-1}$)**	
		For $[Pt_4(2\text{-}atp)_8(H_2O)(OH)]$	**For $[Pt_2(2\text{-}atp)_4(H_2O)(OH)]$**
I	418	18224	9298
II	542	16186	8258
III	614	28696	14641
IV	724	176345	89972
V	832	16472	8404
VI	951	10527	5371

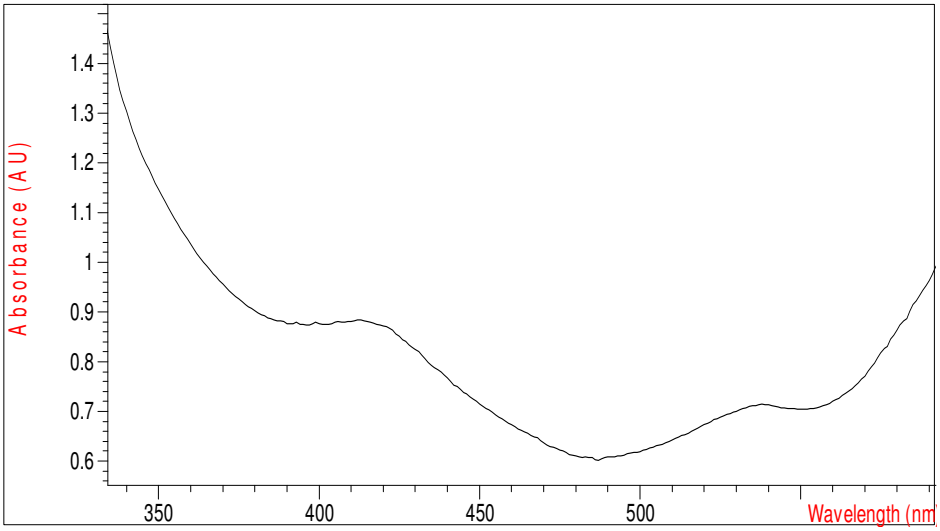

Figure 16. The electronic absorption spectrum of the blue complex in acetone between 330-590 nm ranges. (Concentration based on the formula as $[Pt_2(2\text{-}atp)_4(H_2O)(OH)] = 1.32x10^{-4}$ M).

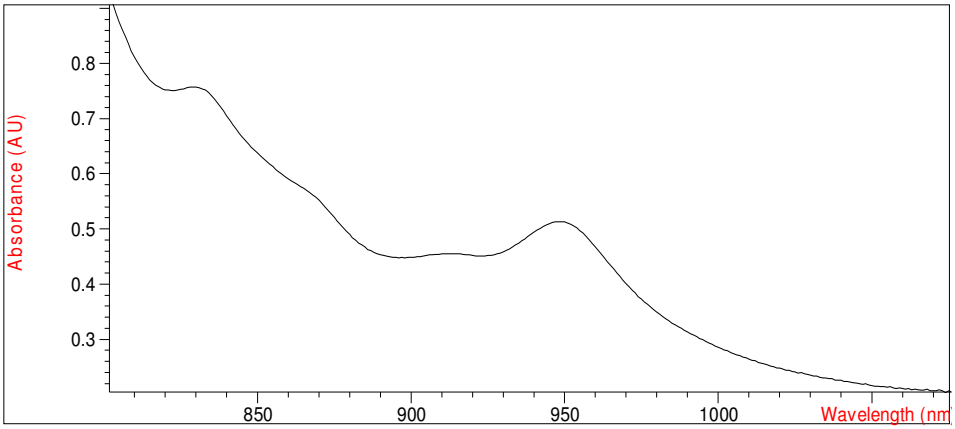

Figure 17. The electronic absorption spectrum of the blue complex in acetone between 800-1000 nm ranges. (Concentration based on the formula as $[Pt_2(2\text{-}atp)_4(H_2O)(OH)] = 1.32x10^{-4}$ M).

The absorption spectrum of the ligand (Figure 14) has two distinct bands at 340 nm and 220 nm. The band at 220 nm is about four times more intense than the one at 340 nm. There are no absorptions in the region of the spectrum λ>400 nm.

The most important feature in the spectrum of the blue complex is the intense band at 724 nm. The energy and the intensity of this band are consistent with previously reported platinum blues [9]. This is the band which is responsible for its blue color. The higher energy part of the spectrum is similar to that of free ligand spectrum, but shifted to little bit higher energy. For example, the band at 340 nm in the free ligand is shifted to 320 nm in the coordinated ligand. It seems very obvious that the absorptions which appear in the higher energy region (λ<400 nm) in the spectrum of the blue complex result from the electronic excitations within the coordinated ligand. Thus the intense band at 724 nm and less intense bands in the two sides of it must result from the excitations involving metal based molecular orbitals. Similar band in $[Pt_2(P_2O_5H_2)_4]^{4-}$ appears at 369 nm with molar absorptivity of 31000 $cm^{-1}M^{-1}$ [46].

To form a base for a better understanding of the origin of the intense absorptions at 724 nm and around it, let us examine possible molecular orbitals which might have been involved in the excitations resulting these bands. The molecular orbitals, which result from the interactions of platinum (II) 5d and 6p orbitals in binuclear HH-$[Pt_2(2\text{-atp})_4]$ complex with C_{2h} symmetry are shown in Figure 18. The lowest energy excitations in this complex is expected from $3b_u$ [σ^* (d_z^2-d_z^2)] to 4ag [$\sigma(p_z\text{-}p_z)$] electron transitions. When the two HH-$[Pt_2(2\text{-atp})_4]$ (Figure 12) dimerizes to form a tetranuclear molecule $[Pt_4(2\text{-atp})_8]$ (Figure 13) in eclipsed configuration, with C_{2h} symmetry (the amines of one unit are across the sulfur of the other) the molecular orbitals which are in axial direction of the binuclear $[Pt_2(2\text{-atp})_4]$ complex, those are $1a_g$, $3b_u$, $4a_g$ and $4b_u$, will overlap to form strongest (with respect to other MO's) bonding interactions. The relative energies of the MO's, which will result from this interaction in the tetranuclear complex, are given in Figure 19. When the tetranuclear complex is mixed valence as "Pt(III) Pt_3(II)", the HOMO orbital, which is designated as $2b_u^1$ in Figure 19, becomes partially filled. This will impart paramagnetism to the blue complex. On the other hand, the energy

of the lowest energy allowed electronic transition ($3b_u \rightarrow 4a_g$) in the binuclear complex will be red shifted in the tetranuclear complex ($2b_u^1 \rightarrow 3a_g^1$). The electronic excitations $2a_g^1 \rightarrow 2b_u^1$ and $2a_g^1 \rightarrow 3b_u^1$ are also allowed transitions. According to the argument put forward above, the most logical assignment for the intense band at 724 nm in the electronic absorption spectrum of the blue complex is $^2B_u \rightarrow {}^2A_g$ ($2b_u^1 \rightarrow 3a_g^1$).

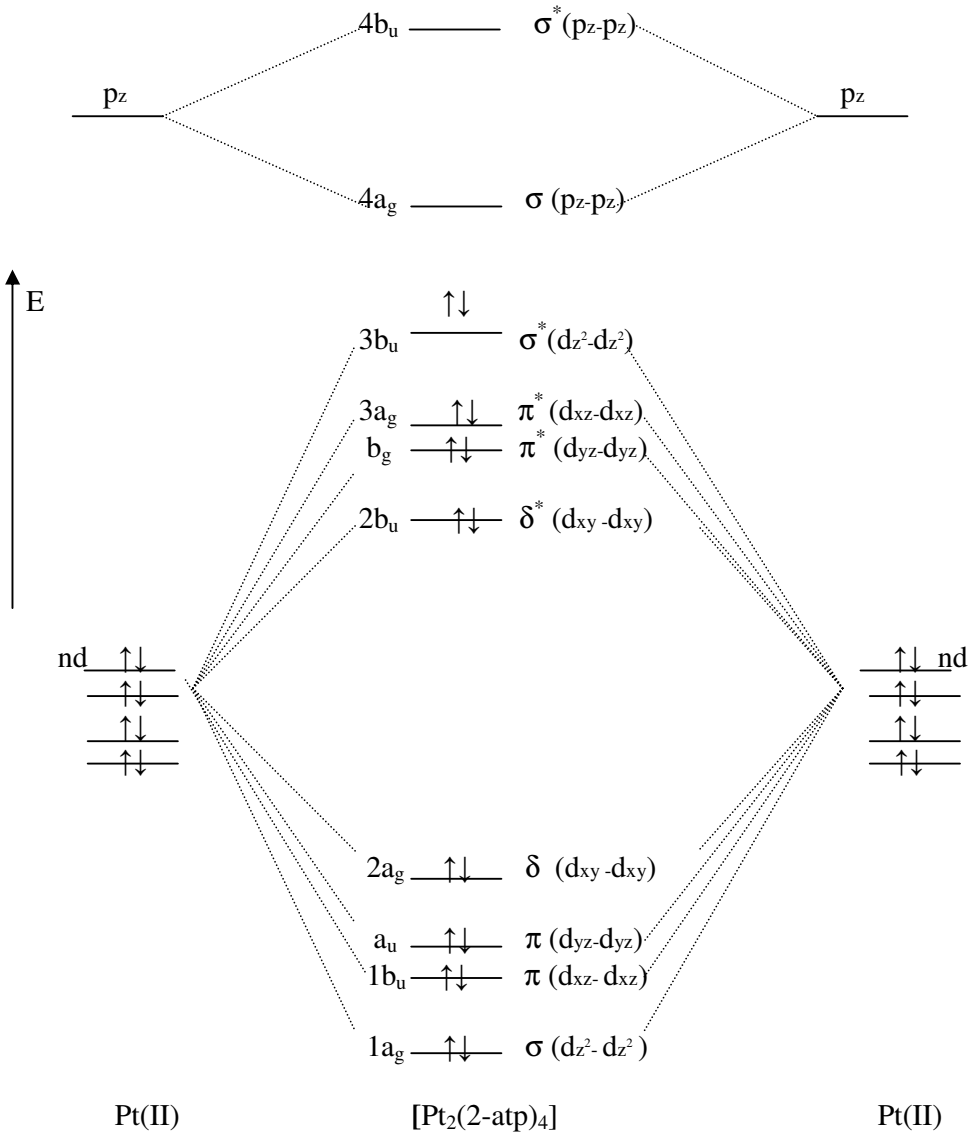

Figure 18. The relative energies and the symmetries of the frontier molecular orbitals of $Pt_2(2\text{-atp})_4$ (C_{2h}).

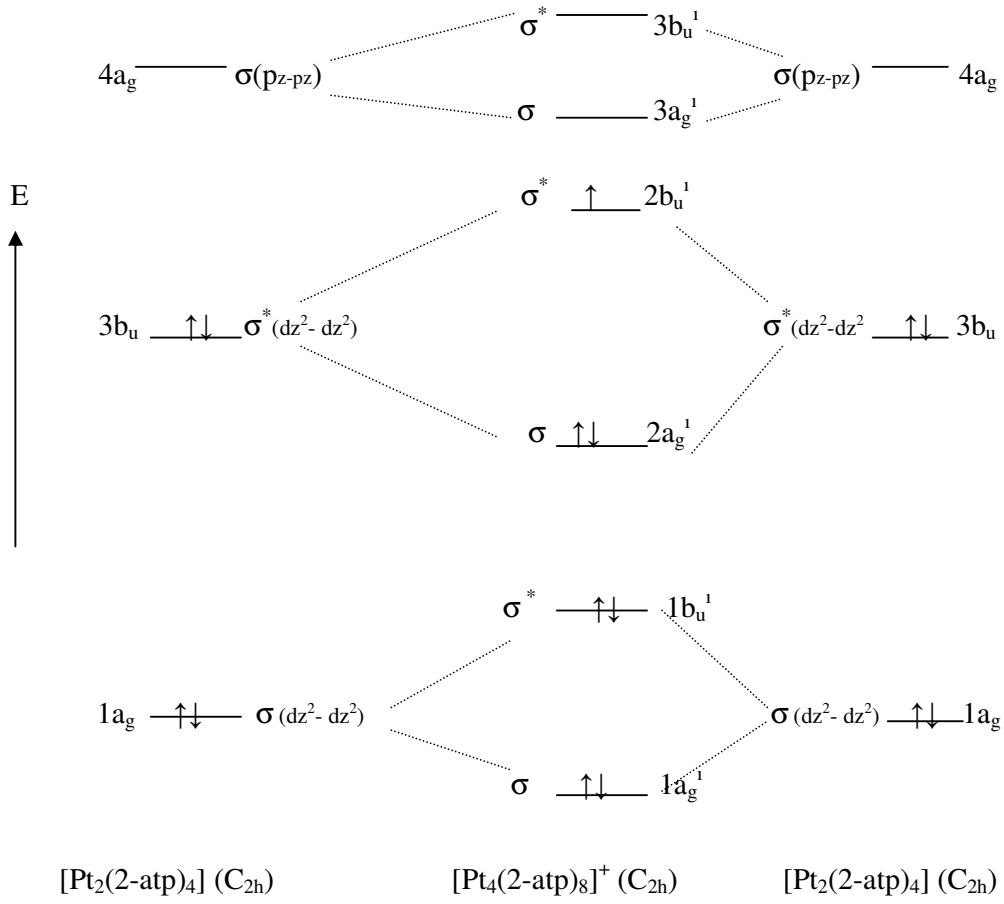

Figure 19. The relative energies and the symmetries of the molecular orbitals which results from two binuclear $[Pt_2(2\text{-atp})_4]$ interaction.

3.1.2. Electron Spin Resonance Spectrum

As explained in section 3.1.1., if the blue complex is a mixed-valence tetranuclear complex, with a metal core "Pt(III) $Pt(II)_3$", it will have an unpaired electron in $2b_u^1$ orbital (Figure 19), thus it must be paramagnetic. $2b_u^1$ orbital is a linear combination of d_z^2 orbitals on four platinum atoms, so the unpaired electron will be delocalized over four platinum atoms.

The ESR spectrum of the α-pyridonate–blue species exhibits an axial signal characteristic of the platinum-blues with $g_{\perp}$ = ~2.4 and $g_{\parallel}$ = ~2.0, where in α-pyridonate–blue Pt-atoms coordinate to nitrogen and oxygen atoms [47, 48, 49, 50]. Similar signal patterns are also observed for several other blue compounds [51, 52, 53, 54, 55, 56] and these common features show that the unpaired electron resides on the d_z^2 orbital located on the Pt chain. Moreover, the detailed investigations of the hyperfine structure revealed that the unpaired electron has interactions with all four ^{195}Pt nuclei within the tetraplatinum chain [50, 57], indicating that the unpaired electron is delocalized over four platinum atoms.

The ESR spectrum of the blue complex in acetone at 150 K exhibited three g values of g_1 = 2.36, g_2 = 2.16 and g_3 = 2.02 (Figure 20). The observed spectral pattern is consistent with the ones reported in literature, except the signal at 2.16. The clear signals indicate that the blue complex has unpaired electron. This result is fully consistent with our predictions.

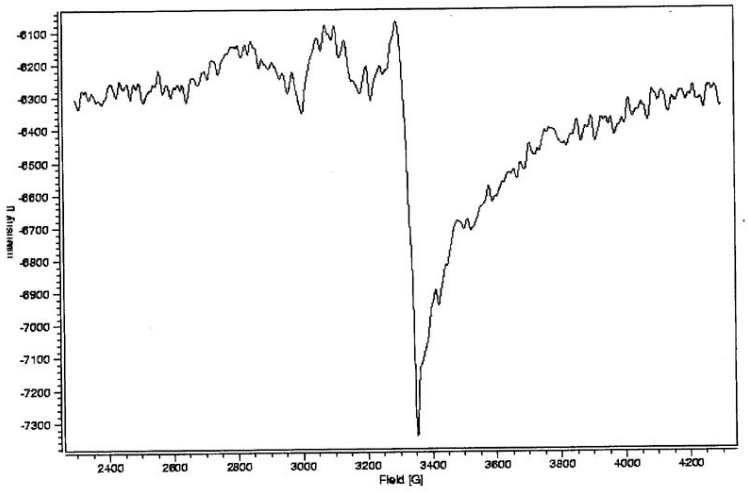

Figure 20. The ESR spectrum of the blue complex in acetone at 150 K.

3.1.3. X-Ray Photoelectron Spectrum of the Blue Complex

X-Ray photoelectron spectroscopy (XPS), is a good means to probe the oxidation state of the metal centers by observing the Pt $4f_{7/2}$ and $4f_{5/2}$ binding energies. The Pt 4f binding energies for the common Pt(IV) compounds are 2-3 eV higher than those for the common Pt(II) complexes. On the other hand, it must always be kept in mind that substitution of the donor ligands can also lead to a shift of 1-2 eV at each peak [9].

The XPS of the blue complex is given in Figure 21. The platinum $4f_{7/2}$ and $4f_{5/2}$ binding energies were obtained at 71.1 and 74.6 eV, respectively. These values were lower than the reported results, for which nitrogen and oxygen donor ligands complexes were examined (Table 4) [9]. The observed shifts in the binding energies of platinum atoms in our complex can be ascribed to the coordination of sulfur donor ligands.

The observation of only two peaks indicates the presence of one type of platinum from the oxidation stand point. This result is consistent with the delocalization of all electrons in d_z^2 based molecular orbitals in the proposed tetranuclear structure for the blue complex.

Table 4. Platinum $4f_{7/2}$ and $4f_{5/2}$ binding energies of some platinum complexes [9].

Chemical Formula	Pt $4f_{5/2}$	Pt $4f_{7/2}$
Cis-$PtCl_2(NH_3)_2$ (Pt(II))	75.4	72.0
HH-$[Pt(2.0+)_2(en)_2(PRI)_2]_2(NO_3)_4$	76.4	73.1
HH-$[Pt(2.25+)_2(NH_3)_4(PRI)_2]_2(NO_3)_5.H_2O$	76.2	72.8
HH-$[Pt(2.5+)_2(NH_3)_4(PRO)_2]_2(NO_3)_6.2H_2O$	76.4	72.9
HH-$[Pt(3.0+)_2(NH_3)_4(PRO)_2(NO_2)(NO_3)]$ $(NO_3)_2.H_2O$	77.9	74.6
The Blue Complex prepared in this work	74.6	71.1

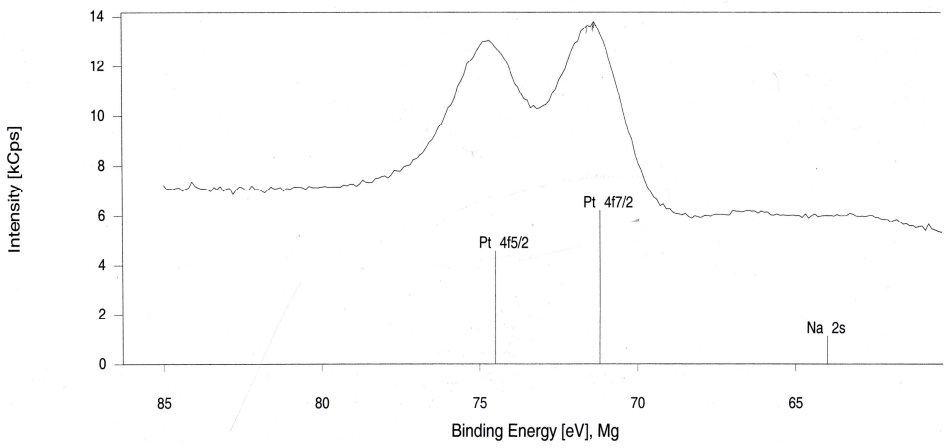

Figure 21. The XPS of the blue complex.

3.1.4. ^{1}H, ^{13}C and ^{195}Pt NMR Spectra

The ^{1}H and ^{13}C NMR spectra of the blue complex (Figure 24, 25) were measured in acetone-d_6 solvent. For the comparison reason, ^{1}H and ^{13}C NMR spectra of the free ligand, H2-atp (Figure 22, 23), were also measured in acetone-d_6. The chemical shift values are tabulated in Table 5.

Table 5. NMR data for H2-atp and the blue complex.

^{1}H-NMR (ppm)	The Blue Complex	δ(N-H)2.7; δ(H1)6.9; δ(H2)7.0; δ(H3)7.3; δ(H4)7.7
	H2-atp	δ(N-H)3.5; δ(S-H)5.2; δ(H1)6.4; δ(H2)6.5; δ(H3)6.7 δ(H4)6.8
^{13}C-NMR (ppm)	The Blue Complex	δ 115.8; δ 117.6; δ 118.3; δ 132.2; δ 137.0
	H2-atp	δ 109.3; δ 119.4; δ 121.7; δ 125.2; δ 126.8; δ 146.8
^{195}Pt-NMR (ppm)		δ –3175

Chemical shifts (δ) are given in ppm, relative to TMS in acetone-d_6.

Careful examination of the chemical shift values indicates that the blue complex do contain 2-aminothiophenol ligand. In the ^{1}H-NMR spectrum of the blue complex, the peak corresponding to the thiol hydrogen at 5.2 ppm is missing, and also the peak corresponding to the amine hydrogens is shifted from 3.5 ppm to 2.7 ppm going from free ligand to the coordinated one. These observations clearly indicate that the H2-atp coordinates to the platinum from sulfur and nitrogen, and it is also anionic.

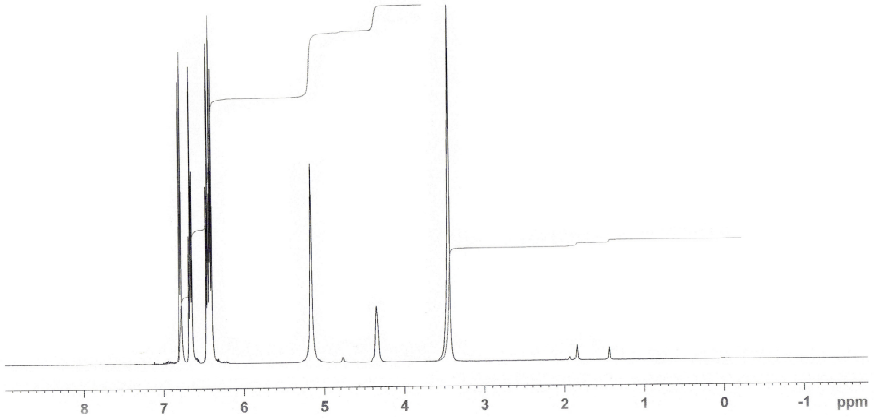

Figure 22. ^{1}H-NMR of H2-atp in acetone-d_6.

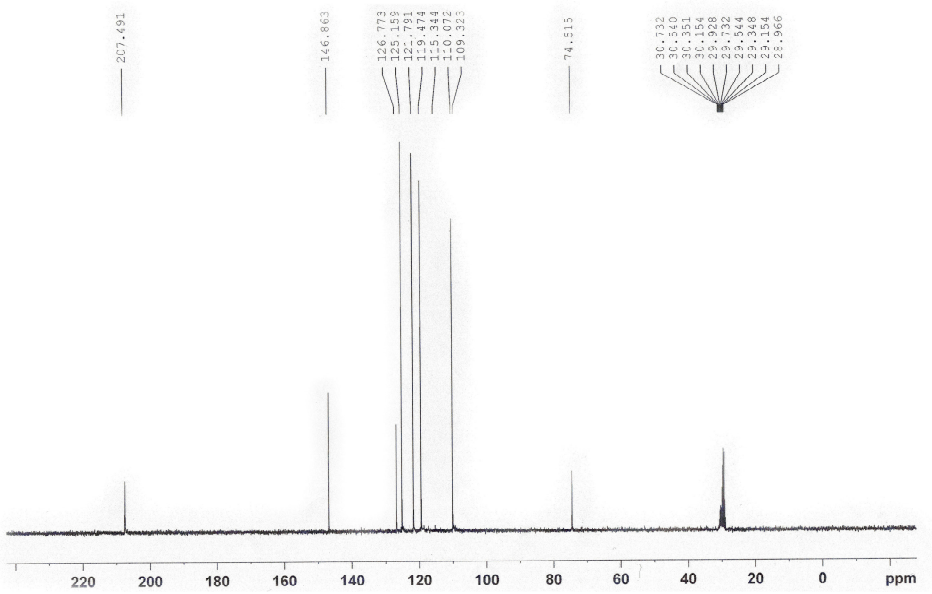

Figure 23. ^{13}C-NMR of H2-atp in acetone-d_6.

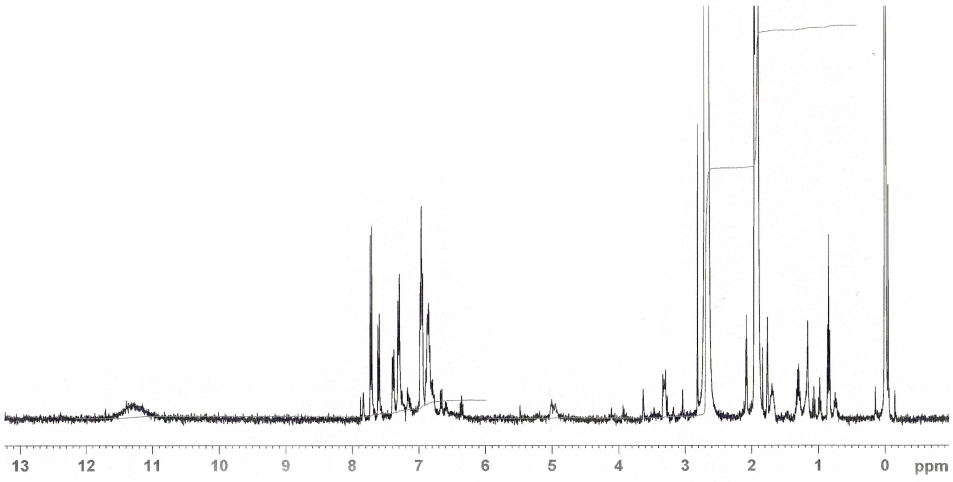

Figure 24. ^{1}H-NMR of the blue complex in acetone-d_6.

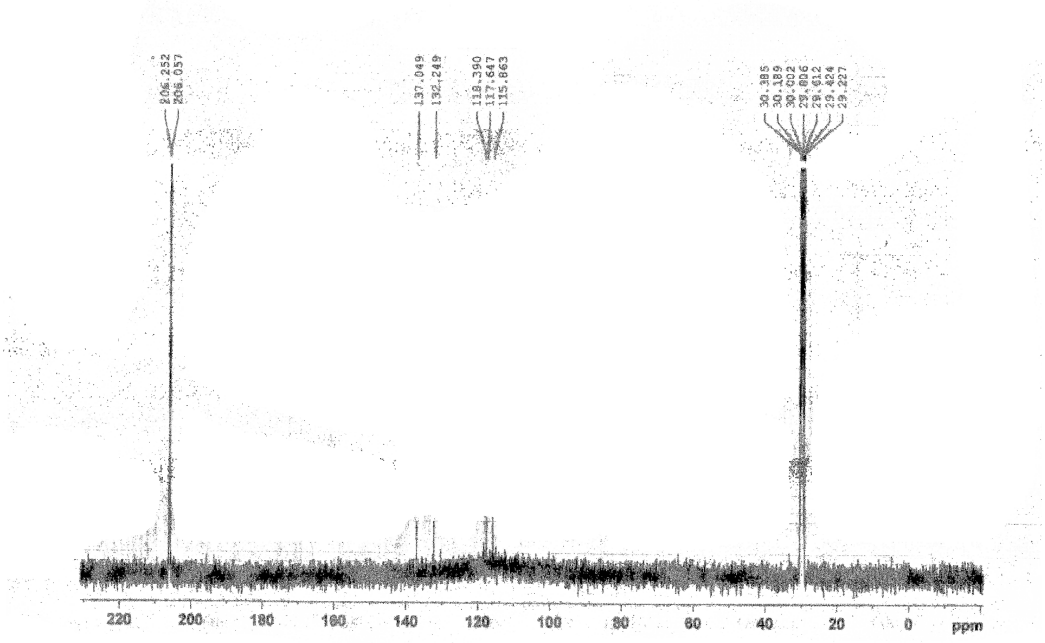

Figure 25. ^{13}C-NMR of the blue complex in acetone-d_6.

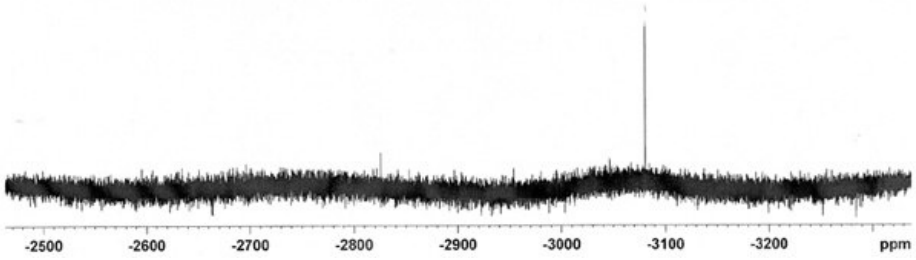

Figure 26. The ^{195}Pt-NMR spectrum of blue product in acetone-d_6.

The ^{195}Pt-NMR spectrum of the blue complex was also measured in acetone-d_6. The spectrum of the blue complex is presented in Figure 26. A signal at -3175 ppm was observed as referenced to K_2PtCl_4 set at "0" ppm, which indicates the presence of two nitrogen and two sulfur atoms around the platinum atom within the range of -3100 and -3200 ppm [9, 58]. Since the blue complex is paramagnetic due to the unpaired electron on the platinum atoms, the ^{195}Pt-NMR spectrum is not reliable.

3.2. Electrochemistry

Electrochemical behavior of the blue complex and the ligand, H2-atp, were studied via cyclic voltammetry (CV) and UV-Vis spectroscopy using platinum (or glassy carbon) electrodes versus SCE (or Ag-wire) in acetone-$[(n\text{-}C_4H_9)_4N]BF_4$ solvent-electrolyte couple. The cyclic voltammetric data are summarized in Table 6.

Table 6. Cyclic Voltammetric data for H2-atp and the blue complex in acetone-$[(n\text{-}C_4H_9)_4N]BF_4$ solvent-electrolyte couple.

Compound	**E_a(V)[a]**	**E_c(V)[b]**	**Reference Electrode**
H2-atp	0.75 1.08	- 0.67	SCE
	0.84 1.26	- 0.42	Ag-wire
The Blue Complex	0.90[c] (72) 1.53	-0.36[c] (50) -1.15[c] (50)	SCE
	1.10[c] (58) 1.67	-0.14[c] (62) -0.92[c] (60)	Ag-wire

[a] Oxidation peak potential; [b] Reduction peak potential.

[c] Reversible peak potential.

Difference between the peak potentials of the reversible peaks were given in parenthesis in mV.

3.2.1. The Blue Complex

The cyclic voltammogram of the blue complex in acetone, displays two oxidations, at 1.10 V (rev) and 1.67 V, and two reversible reduction, at -0.14 V (rev) and -0.92 V (rev), peaks versus Ag-wire reference electrode (Figure 27).

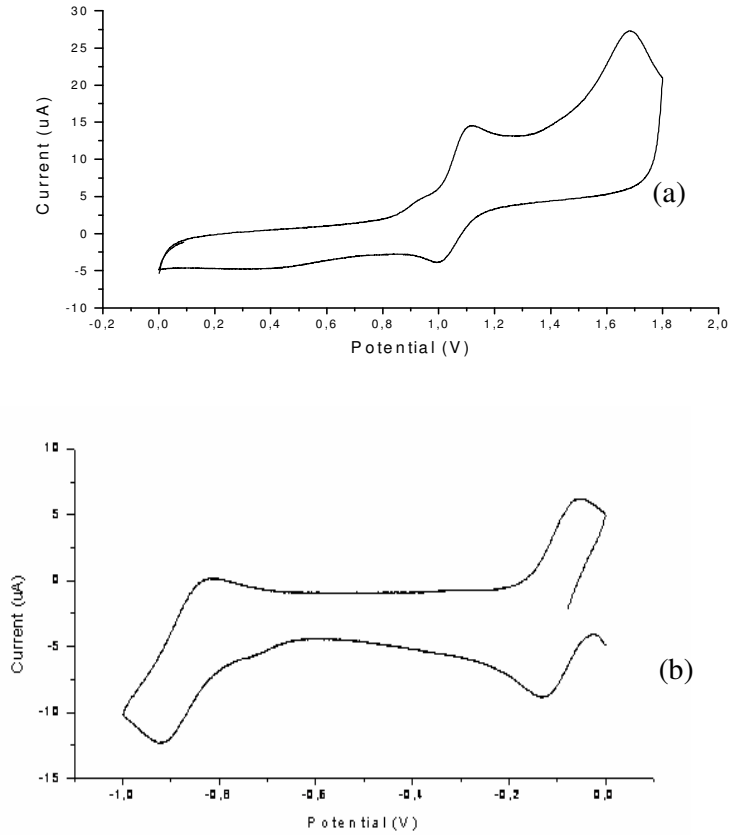

Figure 27. CV of 0.001 M the blue complex in acetone vs Ag-wire. (a) Anodic sweep (b) Cathodic sweep. (Molar concentration is based on the formula $[Pt_2(2\text{-atp})_4(H_2O)(OH)]$)

Controlled potential electrolysis of the blue complex was carried out both at the first and second oxidation peak potentials by chrono-coulometry in order to calculate the number of electrons transferred during the electro-oxidation. The

quantity of the charge is followed with respect to time in chrono-coulometry and the electrolysis at the peak potentials were ended when the coulometric plot reached to the plateau. The calculations, depending on the quantity of charge, indicated one and two electron transfer processes for the 1st and 2nd peak potentials, respectively. The number of the electron transferred during the electrochemical oxidation of the blue complex at the peak potentials was also confirmed by peak-clipping method, where the area under the each wave was integrated and compared with that of the ferrocene/ferrocenium couple, which was in the same concentration of the blue complex.

A plot of the peak current (I_a) versus the square root of the voltage scan rate ($V^{1/2}$) within the range of 100 to 900 mV/s, is given in Figure 28. According to the "Nichelson-Shain" criteria, the positive slope in Figure 28 indicates a diffusion controlled electron exchange reaction at the first oxidation peak potential of the blue complex. The plot of current function $I/(CV^{1/2})$ vs log V gave a straight line parallel to horizontal axis for the 1st oxidation potential indicating a reversible exchange reaction according to "Nichelson-Shain" criteria (Figure 29). Furthermore, the ratio Ipc/Ipa was independent of scan rate and equal to unity for scan rates changing from 100 to 900 mV/s.

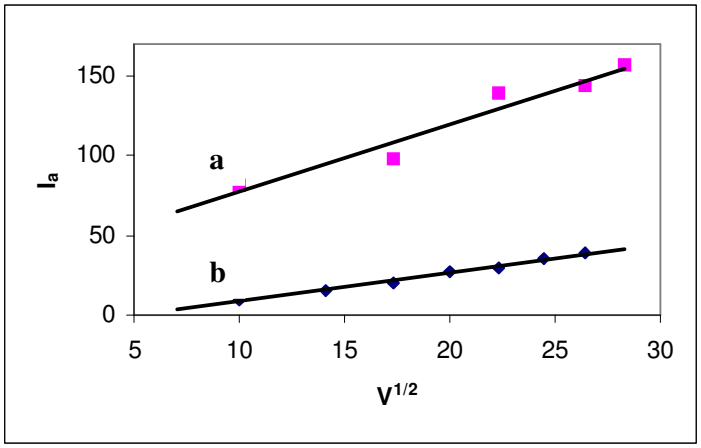

Figure 28. Variation of anodic current (μA) with the square root of voltage scan rate (mV/s). [a] H2-atp; [b] the blue complex.

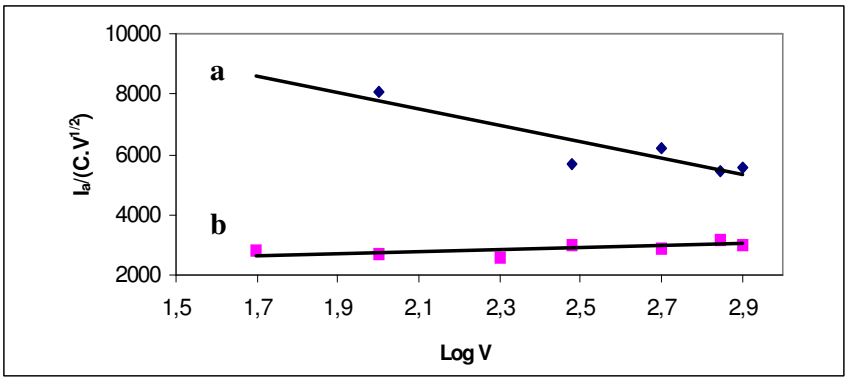

Figure 29. Variation of current function $I/(CV^{1/2})$, with the logarithm of the voltage scan rate plot of H2-atp (a) and the blue complex (b) for the 1st oxidation peaks, where I(μA) is the peak current, V(mV/s) the voltage scan rate and C(mol/L) is the molar concentration.

Constant potential electrolysis of the complex in acetone was performed at the two oxidation peak potentials consecutively, at -5±1 ºC, versus Ag wire. The changes in the electronic absorption spectrum of the blue complex, which were measured in *situ* during the electrolysis, are shown in Figure 30.

The controlled potential electrolysis carried out at the first oxidation peak potential results an increase in the intensity of the band at 724 nm in Figure 30 (a). If the most intense absorption band at 724 nm is assigned to metal to metal electron transfer transition due to the mixed valance character, the increase in the intensity of this band would indicate the formation of more “blue complex” in the electrolyte solution. During the electro-reduction of the blue complex at the same electrode potential, the original complex spectrum was also obtained.

During the electrochemical oxidation at the 2nd oxidation peak potential following the 1st electron transfer, the band at 724 nm diminished indicating the production of unstable Pt(III) species in tetranuclear form (Figure 30 (b)). Then this ($Pt_3^{III}Pt^{II}$) species decomposed completely to an unknown compound at the end of the electrolysis. No new band formation and isosbestic points were obtained during the electron transfer processes at the 1st and 2nd peak potentials.

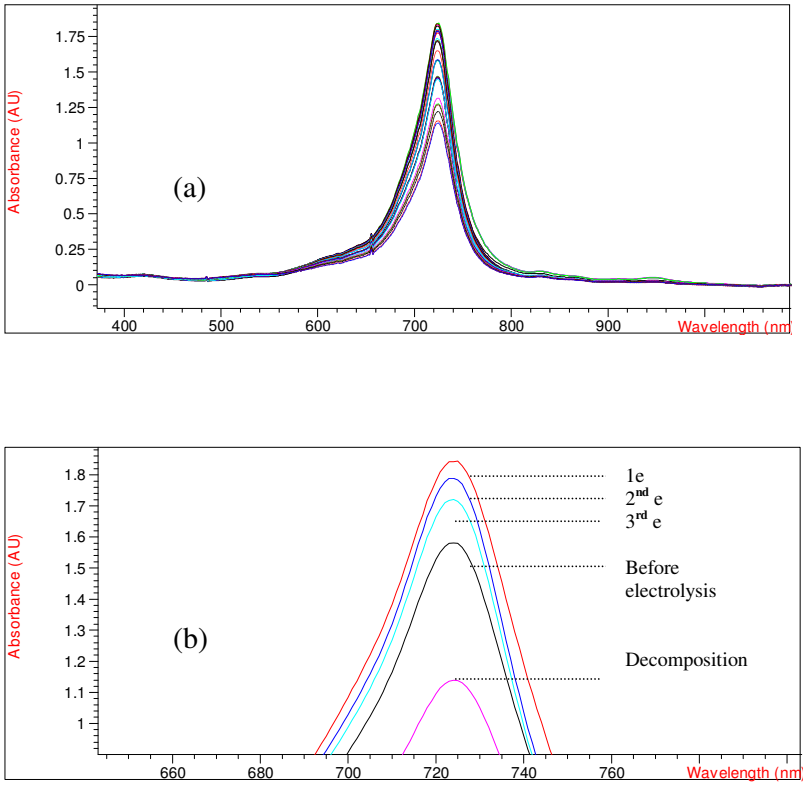

Figure 30. Recorded changes in the electronic absorption spectrum of the blue complex during the constant potential electrolysis in acetone (a) electrolysis at the 1st oxidation peak potential followed by the 2nd peak potential (b) spectral changes obtained at the end of 1st, 2nd and 3rd consecutive e^- transfer.

Consequently, the spectroscopic and coulometric results suggest that the electrochemical oxidation of blue complex at the 1st and 2nd oxidation peak potentials

takes place through the metal center. A possible mechanism for the electrochemical oxidation of the blue complex is as follows;

$$2Pt_2^{II} \rightarrow Pt^{III}Pt_3^{II} + e^- \quad \text{(Ia)} \quad (8)$$

$$Pt^{III}Pt_3^{II} \rightarrow Pt_3^{III}Pt^{II} + 2e^- \quad \text{(IIa)} \quad (9)$$

$$\downarrow$$

Decomposes to an unknown product.

The two reversible cathodic peaks at -0.36 and -1.15 V vs SCE can be assigned as Pt^{III}/Pt^{II} and Pt^{II}/Pt^{I} electron transfer processes, respectively, depending on the coulometric and spectroscopic results.

$$Pt_3^{II}Pt^{III} + e^- \leftrightarrow 2Pt_2^{II} \quad (I_c) \quad (10)$$

$$2Pt_2^{II} + e^- \leftrightarrow Pt_3^{II}Pt^{I} \quad (II_c) \quad (11)$$

Pt^{II}/Pt^{I} electron transfer process was also suggested at around the same peak potential in literature for a mononuclear Pt-complex containing sulfur donor ligand, diethyldithiocarbomate [59].

3.2.2. 2-Aminothiophenol, H2-atp

The cyclic voltammogram of H2-atp was taken in acetone at room temperature, which is shown in Figure 31. As shown in the Figure, CV of ligand consists of two irreversible oxidation peaks at around 0.75 V and 1.08 V and an irreversible reduction peak at -0.67 V vs SCE (Table 6).

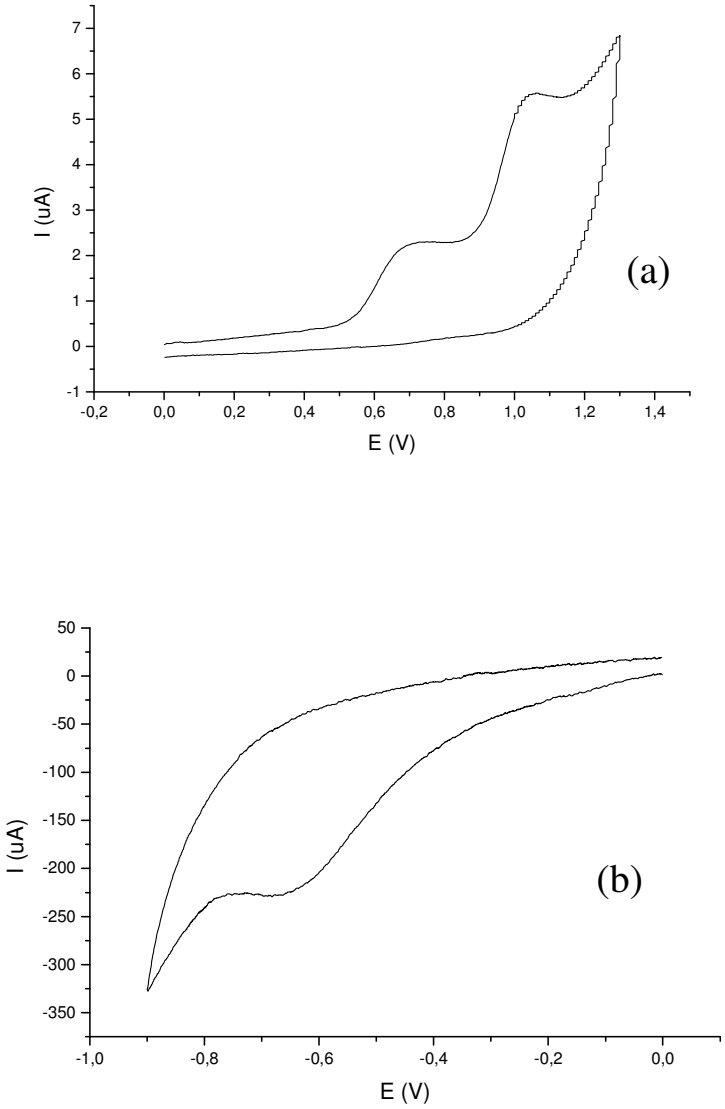

Figure 31. The cyclic voltammogram of H2-atp in acetone vs SCE: (a) Anodic sweep, (b) Cathodic sweep.

Controlled potential coulometry and the peak clipping methods confirmed one electron transfer at the 1st oxidation peak potential and $2e^-$ transfer at the 2nd oxidation peak potential.

According to the "Nichelson-Shain" criteria, the positive slope in Figure 28 indicates a diffusion controlled electron exchange reaction at the first oxidation peak potential of H2-atp. The negative slope of the plot of $I/(CV^{1/2})$ vs log V shows a

reversible electron transfer, which is followed by a chemical reaction (Figure 29). Appearance of irreversible peaks at I_a (Figure 31), instead of a reversible one, can be explained by a fast chemical reaction following the electrochemical one.

Constant potential electrolysis of H2-atp was carried out at 100 mV more positive potentials than the original peak potentials at platinum electrodes vs Ag-wire in acetone-Bu_4NBF_4 solvent-electrolyte couple at room temperature. The spectral changes that occur during the oxidation were followed in situ on a UV-VIS spectrophotometer. The spectral changes during the electrolysis were displayed in Figure 32. During the electrochemical oxidation of H2-atp at the first oxidation peak potential, the band at 355 nm, which is the characteristic band in the spectrum of H2-atp, increase its intensity gradually while a new shoulder at about 499 nm appeared with the change in the color of the electrolyte solution from colorless to pink. No isosbestic point was observed during this process. At the end of the $1e^-$ transfer, the potential was switched to the 2^{nd} oxidation peak potential and the changes in the spectrum were also monitored in *situ* by using UV-VIS spectrophotometer (Figure 33).

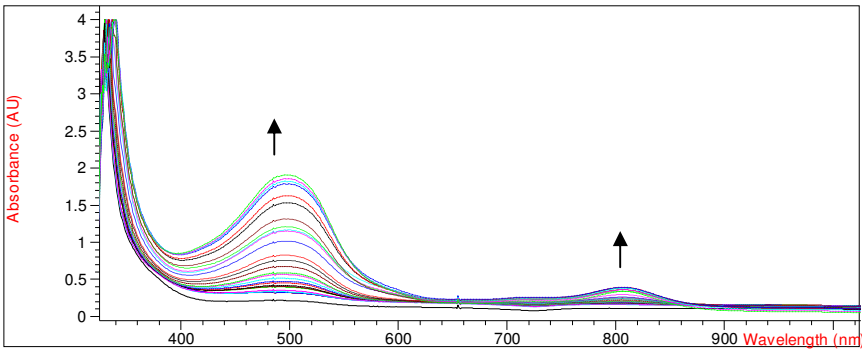

Figure 32. The spectral changes in the electronic absorption spectrum of H2-atp in acetone during the constant potential electrochemical oxidation, at the first and then followed at the second oxidation peak potentials.

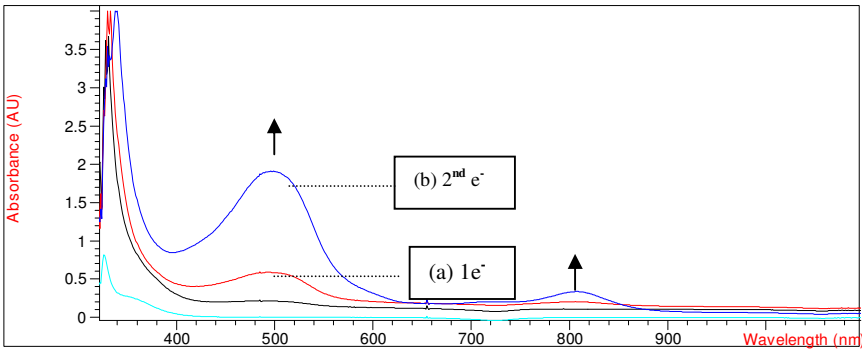

Figure 33. The electronic absorption spectrum of H2-atp in acetone after electrochemical oxidation; (a) after $1e^-$ transfer, (b) after $2e^-$ transfer.

Electrolysis at the 2nd oxidation peak potential showed that the intensity of the shoulder at 499 nm increased and became a peak while the band at 355 nm was much more intense. Moreover, a new band formation was also observed at around 808 nm with two isosbestic points at 656 and 866 nm, indicating one step electrode reaction in the electrolyte solution. Color of the electrolyte solution turned to dark pink at the end of this step and changed to colorless within a few minutes after the electrolysis stopped.

Similar spectral changes were also obtained when the electrolysis carried out at low temperature (-5 ± 1ºC).

In the light of the voltammetric, coulometric and spectroscopic findings, the electrochemical process involving H2-atp in acetone, can be summarized as follow:

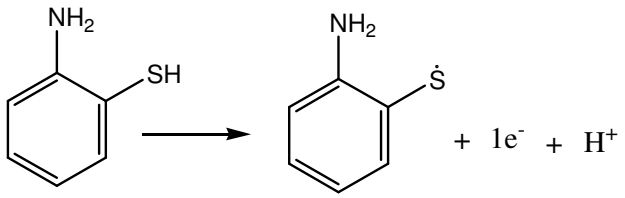

(12)

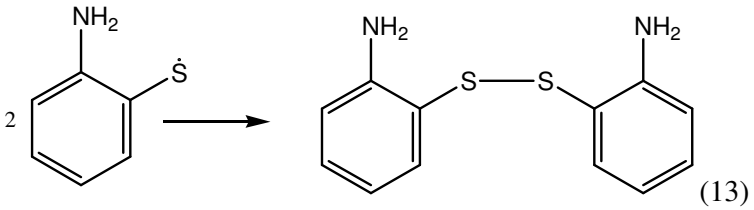

(13)

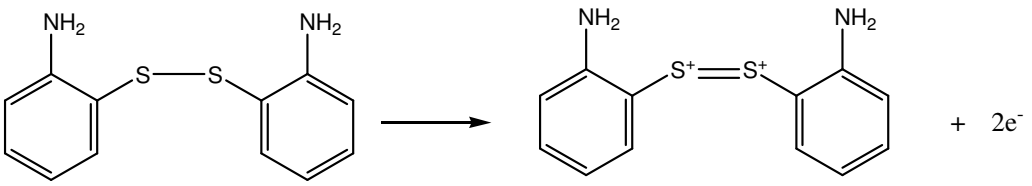

(14)

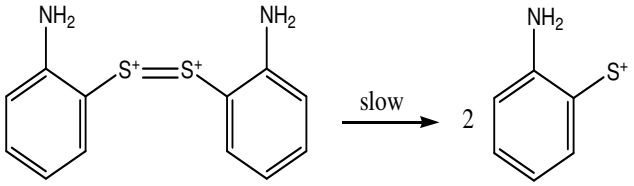

(15)

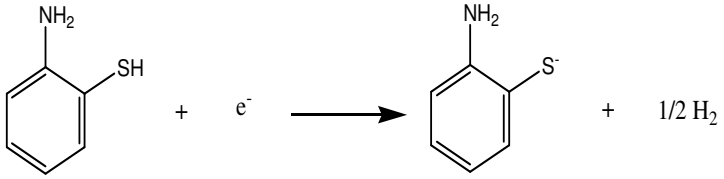

(16)

These observations suggest an oxidation process involving the initial formation of an RS radical as in Equation 12, followed by dimerization to the disulfide (RSSR) as in Equation 13. The disulfide can be afterwards oxidized to

disulfide cation, RS^{+}-^{+}SR, by 2 electron transfer as shown in Equation 14. Then, $RS^{+}S^{+}R$ is slowly decomposed to the sulfenium cation, RS^{+} (Equation 15) [60, 61]. The reduction processes, on the other hand, yielded the thiophenolate ion (RS^{-}) (Equation 16), which was quickly transferred to thiophenol, RSH as a result of attacking of H^{+} present in the electrolyte solution.

All these results indicated that the oxidation and reduction processes took place in the CV of the blue complex are metal based rather than ligand.

CHAPTER 4

DNA BINDING STUDIES

4.1. UV Titration

DNA plays an important role in the life process because it carries heritage information and instructs biological synthesis of proteins and enzymes through the process of replication and transcription of genetic information in living cells.

Interaction of DNA with drugs is one of the important aspects of biological studies in drug discovery and pharmaceutical development processes [62, 63].

Anticancer drugs interact with DNA in different ways. One of them is the intercalation of planar aromatic ring systems between base pairs. Planar organic molecules containing several aromatic condensed rings often bind DNA in an intercalative mode as in the case of DNA-acridine interaction as shown in Figure 34 [64].

Groove binding interaction is the 2nd mode as presented in the Figure 35 for DNA-distamycin [65], in which the drug interacts with two grooves (minor and major) of DNA-double helix. Minor binding causes intimate contacts with the walls of the groove and the numerous hydrogen bonding and electrostatic interactions with the bases and phosphate backbone. Major groove binding causes hydrogen bonding to DNA, forming a DNA triple helix.

The third type of interaction is the electrostatic interaction. Generally metal ion interactions can be given as an example of this kind of interactions [66-68].

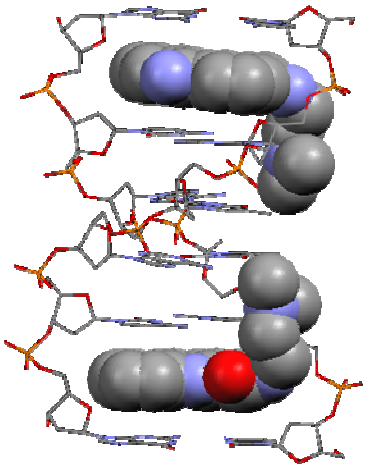

Figure 34. DNA-Acridine interaction as an example of intercalative mode.

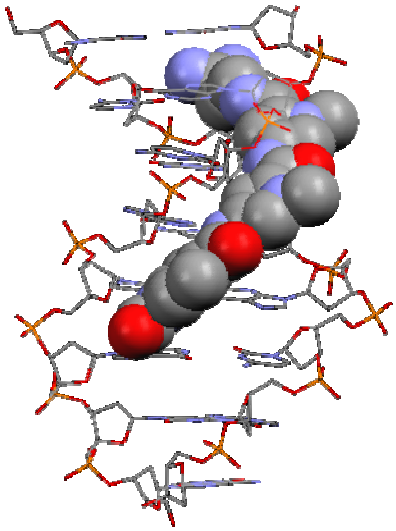

Figure 35. Groove binding of DNA-Distamycin.

The interactions of DNA with nucleic acid binding molecules has been extensively studied by a variety of techniques such as DNA-footprinting [69-70],

NMR [71-72], mass spectrometry [73-79], spectrophotometric methods [80], FTIR and Raman spectroscopy [81-82], molecular modeling techniques [83-85], equilibrium dialysis [86], electric linear dichroism [87-91], capillary electrophoresis [92-96] and surface plasmon resonance (an optical method to measure the refractive index near a sensor surface within 300 nm) [97-100].

Electronic absorption spectroscopy is universally employed to determine the binding of complexes with DNA. In order to determine the DNA binding characteristics of the blue complex, the interaction of complex with calf thymus (ct)-DNA were monitored using electronic absorption spectroscopic titration at room temperature at fixed concentration ($4.33x10^{-5}$ M) of complex and increasing concentrations of DNA ($8.66x10^{-5}$ M (R=2), $1.30x10^{-4}$ M (R=3), $1.73x10^{-4}$ M (R=4), $2.60x10^{-4}$ M (R=6), $3.46x10^{-4}$ M (R=8), and $4.33x10^{-4}$ M (R=10) in tris buffer (50 mM NaCl)-acetone (8:2) mixture at pH=7.1. The blue complex is not soluble in aqueous solution, thus acetone was used to overcome this solubility problem of the complex in tris-buffer solution. Although the electronic absorption spectrum of the blue complex in acetone contains only one intense band at 724 nm, an additional band appeared at about 550 nm upon the addition of the tris buffer solution (Figure 36). Accordingly, an equilibrium was established between the aqueous solvent coordinated and uncoordinated form of the blue complex in tris-acetone mixture. The change in tris buffer-acetone volume ratio disturbed this equilibrium. It was observed that, increasing the volume ratio of tris buffer in this solvent mixture led an increase in the intensity of the band at 550 nm, unlike the band at 724 nm, to a certain extent. Otherwise, sudden precipitation of complex occurred as a result of further dilution with tris-buffer solution. Therefore, the spectroscopic titration of our complex with ct-DNA was made in optimized conditions in which the acetone amount was kept minimum.

Complex bound to DNA through intercalation usually results in hypochromism (decrease in molar absorbance) and red shift (bathocromism), due to the intercalative mode involving a strong stocking interaction between aromatic chromophore and the base pairs of DNA. The extent of the hypochromism is commonly consistent with the strength of intercalative interaction [101-103]. In

contrast, an increase in molar absorptivity (hyperchromism) about 17.5% with an insignificant red shift may be ascribed as the weak binding of the blue complex involving hydrogen bonding interaction between hydroxyl group attached to the complex, when interacted with DNA, or may support the electrostatic binding of ct-DNA (Figure 36). However, the exact binding modes can be defined only if the crystal structures of the complex-DNA adduct are determined. The similar hyperchromism has been observed for porphyrins [104] and 1,3,5,8,10,12-hexaazocyclotetradecane containing macro cyclic Cu[II] complexes and penta coordinated Co(II) complexes containing 1,8-dihydro-1,3,6,8,10,13-hexaazocyclotetradecane containing macro cyclic Cu(II) complexes [105-106].

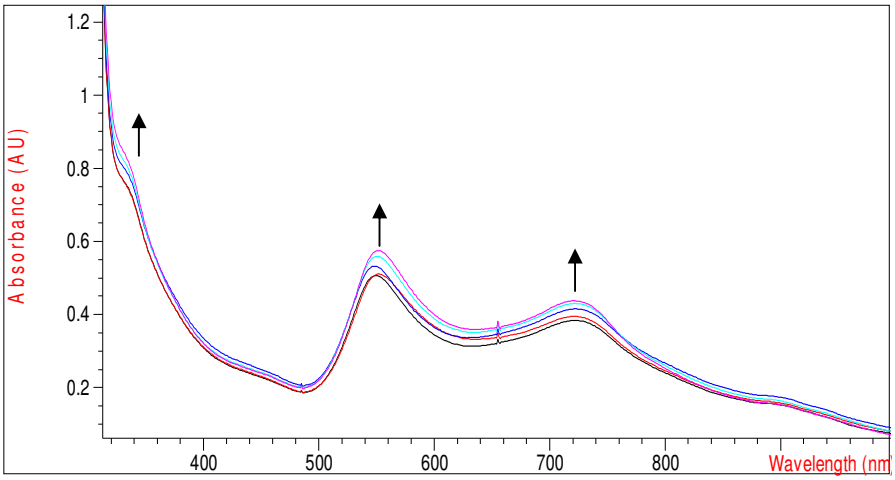

Figure 36. UV titration of the blue complex in 5 mM tris buffer (50 mM NaCl-acetone (8:2) mixture at pH 7.1 where R=2 to 10).

For the blue complex, the intrinsic binding constant, K_b, was determined from the spectroscopic titration data using Equation 17.

$$[DNA / [\varepsilon_A - \varepsilon_F]] = [DNA] / [\varepsilon_B - \varepsilon_F] + 1 / K_b[\varepsilon_B - \varepsilon_F] \quad (17)$$

Where ε_A, ε_F and ε_B correspond to A(abs)/ [Pt], the extinction coefficient for the free platinum complex and the extinction coefficient for the platinum complex in

the fully bound form; respectively. In the plot of [DNA] / [$\varepsilon_A - \varepsilon_F$] versus DNA (Figure 37), K_b is then calculated by the ratio of the slope to intercept. The binding constant obtained for the complex was 5 x 10^{-4}. This K_b value much lower than those observed for typical classical intercalators (ethidium-DNA 1.4 x 10^6 M^{-1}) is also indicative of binding of complex with DNA with a weak interaction such as hydrogen bonding or electrostatic mode.

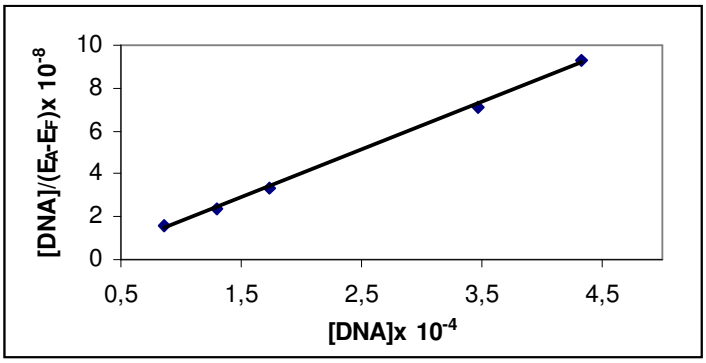

Figure 37. UV titration of the blue complex with DNA for R= 2, 3, 4, 8, 10 values in tris buffer–acetone mixture (8:2).

4.2. Voltammetric Titration

In recent years, there has been a growing interest in the electrochemical investigations of interaction between anticancer drugs and DNA. One of the practical applications of electrochemistry is the determination of electrode redox processes. Due to the existing a distinct parallelism between electrochemical and biological reactions it can be assumed that the redox mechanisms taking place at the electrode and in the body share similar principles [107-108].

Electrochemical investigations of nucleic acid binding molecules-DNA interactions can provide a useful complement to the spectroscopic methods, e.g.

spectroscopically inactive species yield information about the mechanism of intercalation and the conformation of anticancer drug- DNA adduct [109].

The explanation of the mechanism of interaction between anticancer drugs and DNA by electrochemical methods is mainly based on the electrochemical behavior of the anticancer drugs in the presence or absence of DNA. Observation of the electrochemical signal related to DNA-DNA interactions or DNA-drug interactions can provide evidence for the interaction mechanism, the nature of the complex formed, binding constants and the role of free radicals generated during interaction in the drug action. For the electrochemical detection of interaction between drug and DNA, drug should be redox active.

The changes as a dramatic decrease/increase at the peak currents of the drug which selectively binds with double stranded (ds)-DNA or that of the electroactive DNA-bases such as guanine or adenine and the shifts of the formal potentials of the redox couple caused by the intercalation of nucleic acid binding molecules into ds-DNA, are used to determine the action mode of drug to DNA.

Drug- DNA interactions are investigated by using different electrochemical techniques, including cyclic voltammetry [110], square wave voltammetry [111-112], differential pulse voltammetry [113], and chronopotentiometry [114]. The interaction mechanism can be investigated in three different ways, i.e., DNA modified electrode, drug modified electrode and interaction in solution [115].

In this study the interaction of the blue complex with DNA is investigated in solution (Tris buffer at pH=7) where complex and calf thymus (ct)-DNA are placed in the same solution and after some given time of interaction (15 minute), the changes in the electrochemical signals of complex-DNA compound are compared with the signal of complex alone by using cyclic voltammetry. The cyclic voltammogram of the blue complex in aqueous solution (tris buffer at pH=7) displayed two waves at about 0.64 V (quasireversible) for Pt^{II}/Pt^{III} and 1.18 V for Pt^{III}/Pt^{IV} couples versus Ag wire; as shown in Figure 38. This significant change in oxidation potential in aqueous medium towards less positive values (Table 7) is most

probably due to the differing interactions of the solvent to the complex, since water has better hydrogen bonding capability than acetone. In aqueous solution, the platinum redox potentials are lower than that observed in acetone medium.

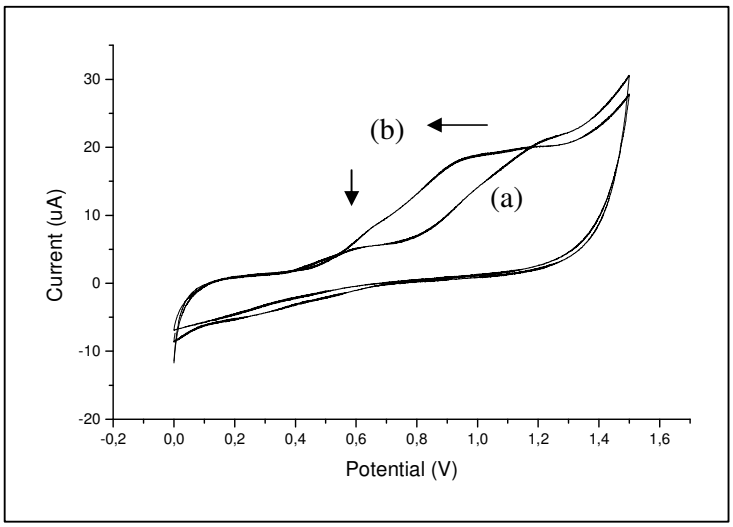

Figure 38. CV of the blue complex (a) in the absence (b) in the presence of DNA in 5 mM tris buffer (50 mM NaCl-acetone (8:2) mixture at pH 7.1 where R=0 and 5)

In the presence of DNA, reversibility of the electron transfer was not maintained. The positive shift in the 1st oxidation peak potential with increasing ratio of total concentration of DNA to blue product suggests a difference in the binding properties of Pt^{II}/Pt^{III} species to DNA.

From reversible redox reactions of the free and bound species, the ratio of the corresponding equilibrium constants for binding of each oxidation is calculated by the Nernst Equation (18) [101-103].

$$E_b^\circ - E_f^\circ = 0.0591 \log [K_{+2}/K_{+3}] \qquad (18)$$

where E_b^o and E_f^o are the peak potentials of bound and free complex, respectively. K_{+2} and K_{+3} are the corresponding binding constants for Pt^{II} and Pt^{III} species to ct-DNA. For the blue product, the K_{+2}/K_{+3} is found to be 0.0966 where E_b = 0.58 V and E_f = 0.64 V. The K_{+2}/K_{+3} value of the complex is less than unity, suggesting preferential stabilization of Pt^{III} over Pt^{II} on binding to DNA. In addition to the changes in formal potential upon addition of ct-DNA, the voltammetric current decreases (Figure 38), which can be attributed to the slow diffusion of the metal complexes bound to the large, slowly diffusing DNA molecules [116].

$$\begin{array}{ccc} [Pt^{II}\text{-}Pt^{III}] & \rightleftharpoons & Pt^{III}\text{-}Pt^{III} + e^- \\ K_{+2} \uparrow\downarrow & & K_{+3}\uparrow\downarrow \\ [Pt^{II}\text{-}Pt^{III}]\text{-DNA} & \rightleftharpoons & [Pt^{III}\text{-}Pt^{III}]\text{-DNA} + e^- \end{array}$$

Under the assumption of reversible diffusion-controlled electron transfer [117], non-linear regression analysis of experimental data was performed by using following equations [118].

$$I_t = B\,[X_f\, D_f^{1/2} + X_b\, D_b^{1/2}] \qquad (19)$$

$$B = 2{,}69 \times 10^5 .n^{3/2} .A\,.\,V^{1/2} \qquad (20)$$

where I_t is the total anodic/cathodic peak current, A is the area of the working electrode [7.85 x 10^{-7} m^2], n is the number of electrons [$1e^-$] involved in the redox reaction, V is the scan rate [100 mV/s], X_f and X_b are the mole fractions of free and bound species to DNA respectively.

A summary of the titration results is given in Table 7. D_b is calculated by using a general assumption in which describing D_b as 6.4% of D_f value [119-120]. D_f and D_b are diffusion constants of free and bound species, respectively.

Table 7. Voltametric and UV titration data for the blue complex with ct-DNA.

Complex	D_f (10^{-4})	$D_b(10^{-5})$	$K_b(10^{-4})$	K_{2+}/K_{3+}
The Blue Complex	2.90	1.85	5.00	0.0966

4.3. Enzyme Activity of the Blue Complex

Human beings ingest number of foreign chemicals, collectively referred to as XENOBIOTICS (xeno means foreign). These include pharmaceuticals, pesticides, herbicides and industrial chemicals as well as complex structures. Many of them insoluble in water, but soluble in fat and therefore tend to participate into the hydrocarbon layer of membranes. Against to the wide range of xenobiotics, organisms have developed several defense mechanisms such as drug efflux pumps, drug sequestration, drug metabolism, and repair of drug-target sites. The vital function of the chemical defense is known as detoxification and is affected principally by the liver.

Detoxification of xenobiotics is one of the major functions of reduced glutathione (GSH). Toxic electrophiles conjugate with GSH, either spontaneously or enzymatically in Glutathione S-transferases catalyzed reactions.

Glutathione S-transferases (GSTs) are enzymes that participate in cellular detoxification of endogenous as well as foreign electrophilic compounds.

$$GSH + RX \rightarrow GSR + HX \qquad (21)$$

Thus, transferase reactions are the major pathway for GSH utilization in the liver. GSTs are found in all human tissues. Normal levels of GSH in humans are 10-30 μM (plasma) 1-3 μM (urine), 3 mM in kidney and 1-10 mM in tumors of various organ sites [121].

Six different classes of soluble GSTs have been identified; alpha (α), mu (μ), pi (π), sigma (σ), theta (θ) and zeta (δ). This classification is in accordance with the substrate specify, chemical affinity, structure, aminoacid sequence and kinetic behavior of the enzyme [122].

The expression level of the different classes of GST is tissue specific, in human liver. The GST alpha class forms 80 % of the total GST expressed and the GST A1-1 isoform predominates. In contrast, human colonic tissue expressed GST pi as the major class of GST.

Differential expression also occurs within an organ, eg: in the kidney, GST alpha predominates in the proximal tubules, whereas GST pi and GST mu are the major isoforms in the thin loop of Henle, the distal tubules and the collecting ducts [123].

The GST in addition to their enzymatic activities, bind with high affinity to a variety of hydrophobic compounds such as heme, billirubin, hormones and drugs, which suggests that may serve as introcellular carrier proteins for the transport of various ligands. A marked increase in GST activity has been observed in tumor cells resistant to anticancer drugs [124]. It has also been shown that alterations in GST and GST levels are related not only in vitro drug resistance but also to clinical response to chemotherapy [123].

In our study, enzyme activity of the blue complex was determined by following the changes on total GST activity in sheep liver with the addition of different concentrations of complex solution prepared in phosphate buffer at pH 6.5. 1-chloro-2,4-dinitrobenzene (CDNB) was used as a substrate which is known as the universal substrate for GSTs since it is used for the demonstration of multiple forms of GSTs in various biological species. When conjugated with GSH, it gives S-(2,4-dinitrophenyl) glutathione, a compound possessing an absorbance spectrum sufficiently different from that of CDNB to allow a simple spectrophotometric assay at 340 nm [41].

Therefore, the GST activity is determined spectroscopically against the substrate CDNB at room temperature by monitoring the formation of the conjugation product.

As demonstrated in Figure 39 clearly, the blue complex inhibits the GST enzyme activity in sheep liver drastically between 45 and 200 μM. A plot of fractional GST enzyme activity versus concentration of the blue complex shows approximately 45 % decrease in the enzyme activity between 45 and 200 μM (Figure 40).

As indicated before, GST enzymes besides their functions of detoxification are also responsible for drug resistance. Inhibition of this enzyme with the blue complex suggests that this complex can be used in combined chemotherapy to increase the drug efficacy.

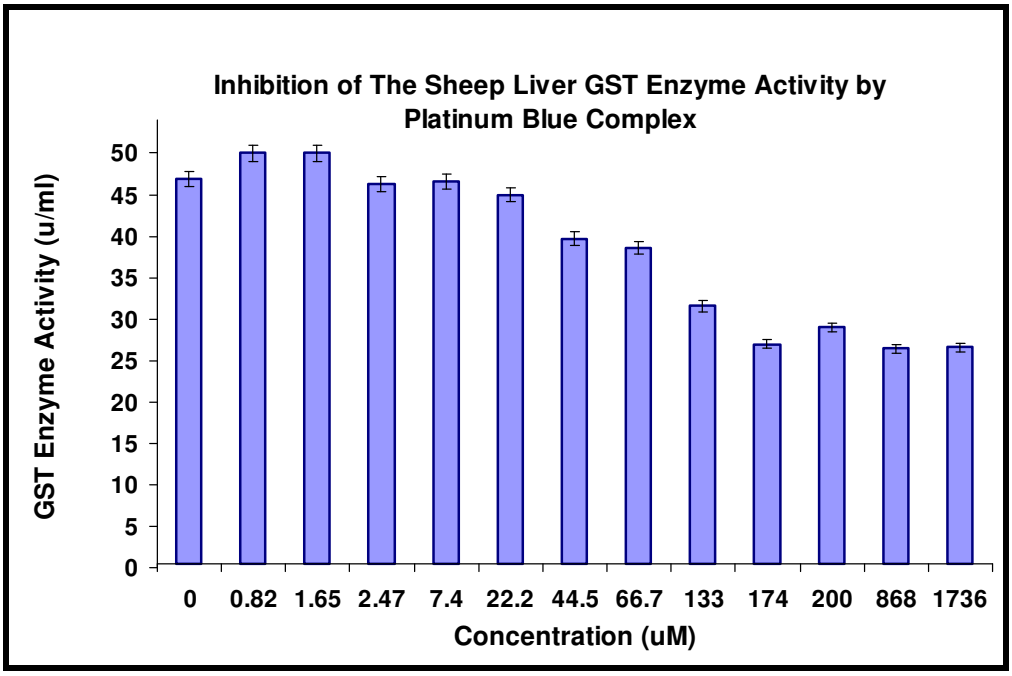

Figure 39. Inhibition of the sheep liver GST enzyme activity by the blue complex.

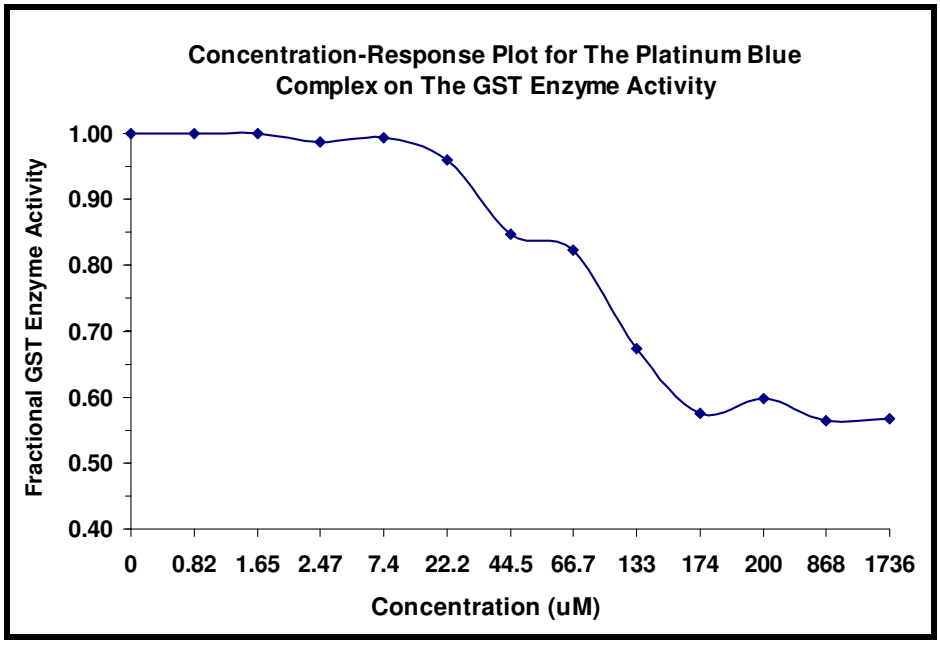

Figure 40. Concentration-response plot for the blue complex on the GST enzyme activity.

CHAPTER 5

CONCLUSION

Reaction of K_2PtCl_4 with 2-aminothiophenol (H2-atp), in basic aqueous solution yielded, first a yellow solid, then, followed by refluxing at around 40ºC yielded a green, and finally a blue solid product. Elemental analysis of all three products suggested that the platinum to 2-aminothiophenolate ratio is 1:2 in all three solids. Among these three, only the blue product, which we call it "the blue complex", was soluble in acetone, acetonitrile, DMSO and DMF. The blue complex is stable in solution and exhibited very strong electronic absorption band at 724 nm. ESR measurement of the blue complex indicated that it is paramagnetic.

On the bases of the results gathered from elemental analysis, UV-Vis, ESR, XPS, ^{1}H-, ^{13}C- and ^{195}Pt-NMR, CV measurements it is proposed that the blue complex is a new "platinum blues", first time synthesized in this work, with a formula $[Pt_4(2\text{-atp})_8(OH)(H_2O)]$. The structure can be visualized as the dimer of the head-to-head isomer of binuclear $[Pt_2(2\text{-atp})_4]$ complex. It is a mixed valence complex with one platinum "+3" and the other three platinums "+2" oxidation state in tetranuclear unit "Pt(III) $Pt(II)_3$". The 2-aminothiophenolate ligand act as bridging ligand coordinating to one platinum from the nitrogen and to the other platinum from the sulfur in a binuclear unit. Dimerization of the binuclear complexes took place with partial oxidation of the metal center yielding a mixed valence tetranuclear complex, in which relatively strong hydrogen bonding type interaction exist between the amine hydrogens of one binuclear unit and the lone pair electrons on the sulfur atom of the other.

The molecular orbital consideration clearly indicates that going from binuclear complex to the tetranuclear complex, the energy of the electronic transition involving metal based molecular orbitals will shift to lower energy part of the

spectrum. The assignment of the electronic transition resulting the distinct 724 nm band is done as $^2B_u \rightarrow {}^2A_g$ ($2b_u^1 \rightarrow 3a_g^1$) (Figure 19).

All platinum blues reported in the literature so far contains nitrogen and oxygen donor atom ligands. The blue complex prepared in this work is the first example of the platinum blues, which contain nitrogen and sulfur donor ligands. It is also interesting that in all previous platinum blues the bridging ligand forms 5-membered ring upon coordination (two platinum atoms and three ligand atoms), in our case the bridging ligand forms 6-membered ring upon coordination. It will be interesting to determine the Pt-Pt distance and compare it with others. Unfortunately, all efforts to prepare a single crystal of the blue complex, appropriate for x-ray analysis, failed. The result of the x-ray structure determination must be ultimate goal in the continuation of this work. This will be the best way to check all hypotheses made on the blue complex in this work.

Electronic absorption spectroscopy is employed to determine the binding mode of the blue complex to ct-DNA. Hyperchromism about 17,5 % with an insignificant red shift revealed a weak binding of the blue complex to DNA, such as electrostatic interaction of metal ions or H-bonding through the hydroxyl group of the complex. The binding constant obtained for the complex was $5x10^{-4}$ which is lower than those observed for classical intercalators, is also indicative of weak binding mode of the blue complex. Voltammetric titration carried out in solution suggested the preferential stabilization of Pt(III) to Pt(II) and Pt(IV) to Pt(III) on binding to DNA.

Enzymatic activity of the blue complex was determined in sheep liver GST enzymes spectroscopically. The blue complex inhibits the GSTs activity between 45-200 μM. Since GST enzymes besides their function of detoxification are also responsible for drug resistance, inhibition of this enzyme with the blue complex suggest that this complex can be used in combined chemotherapy, as well.

REFERENCES

[1] Lippert, B., Coord. Chem. Rev., 1999, 182, 263.

[2] Thompson, D.T., Chem. Br. (1984) 333.

[3] Young, G., Natl. Geogr. 164 (1983) 686.

[4] B. Rosenberg, L. VanCamp, Nature 205 (1965) 698.

[5] B. Rosenberg, L. VanCamp, J.E. Trosko, V.H. Mansour, Nature 222 (1969) 385.

[6] H.M. Pinedo, J.H. Schornagel (Eds.), Platinum and Other Metal Coordination Compounds in Cancer Chemotherapy, Plenum Press, New York, 1996.

[7] S.J. Lippard, Science 261 (1993) 699.

[8] Tejel, C., Ciriano, M.A., Oro, L.A., Chem. Eur. J., 1999, 5, 1131

[9] Matsumoto, K., Sakai., Adv. Inorg. Chem., 2000, 49, 375

[10] Hoffmann, K.A., Bugge, G., Berichte., 1908, 41, 312

[11] Gillard, R.D., Wilkinson, G., J. Chem. Soc., 1964, 2835

[12] Schmuckler, G., Limoni, B., J. Inorg. Nucl. Chem., 1977, 39, 137

[13] Flynn, C. M., Viswanthan, T. S., Martin, R. B., J. Inorg. Nucl. Chem., 1977, 39, 347

[14] Laurent, M. P., Tewksbury, J. C., Krogh-Jespersen, M.B., Inorg. Chem., 1980, 19, 1656

[15] Arrizabalaga, P., Castan, P., Laurent, J. P., Trans. Met. Chem., 1980, 5, 204

[16] Burness, J. H., Inorg. Chim. Acta., 1980, 44, L49

[17] Ettorre, R., Inorg. Chim. Acta., 1980, 46, L27

[18] Allen Chan, C., Marcotte, R. B., Patterson, H. H., Inorg. Chem., 1981, 20, 1632

[19] Laurent, J. P., Lepage, P., Can. J. Chem., 1981, 59, 1083

[20] Laurent, J. P., Lepage, P., Castan, P., Arrizabalaga, P., Inorg. Chem. Acta., 1982, 67, 31

[21] Arrizabalaga, P., Castan, P., Laurent, J. P., J. Am. Chem. Soc., 1984, 106, 1300

[22] Arrizabalaga, P., Castan, P., Laurent, J. P., J. Am. Chem. Soc., 1984, 106, 4814

[23] Rosenberg, B., Van Camp, L., Krigas, T., Nature (London), 1965, 205, 698

[24] Rosenberg, B., Van Camp, L., Trosko, J. E., Mansour, V. H., Nature (London), 1969, 222, 385

[25] Rosenberg, B., Van Camp, L., Cancer Res., 1970, 30, 1799

[26] Hill, J. M., Loeb, E., Mclellan, A., J. Cancer Chemother. Rep., 1975, 59, 589

[27] Davidson, J. P., Faber, P. J., Fisher. R. G., Cancer Chemother. Rep., 1975, 59, 287

[28] Rosenberg, B., Van Camp, L., Krigas, T., Nature (London), 1965, 205, 698

[29] Barton, J. K., Rabinowitz, H. N., Szalda, D. J., Lippard, S. J., J. Am. Chem. Soc., 1977, 99, 2827

[30] Barton, J. K., Rabinowitz, H. N., Szalda, D. J., Lippard, S. J., Waszczak, J. V., J. Am. Chem. Soc., 1979, 101, 1434

[31] O'Halloran, T.V., Lippard. S.J., J. Am. Chem. Soc., 1983, 105, 3341.

[32] O'Halloran, T.V., Lippard. S.J., J. Am. Chem. Soc., 1989, 28, 1289.

[33] Hollis, L.S., Lippard. S.J., Inorg. Chem., 1983, 22, 2605.

[34] Hollis, L.S., Lippard. S.J., Inorg. Chem., 1982, 21, 2116.

[35] Matsumoto, K., Harashima, K., Inorg. Chem., 1991, 30, 3032.

[36] Sakai, K., Matsumoto, K., J. Am. Chem. Soc., 1989, 111, 3074.

[37] Sakai, K., Matsumoto, K., Nishio, K., Tokisue, Y., Ito, R., Nishide, T., Shichi, Y., J. Am. Chem. Soc., 1992, 114, 8110.

[38] Sakai, K., Matsumoto, K., Nishio, K., Chem. Lett., 1991, 1081.

[39] Gillham, B., Biochem. J., 1971, 121, 667.

[40] Habig, W.H., Jakoby, W.B., Methods Enzymol., 1981, 77, 398.

[41] Habig, W.H., Pabst, M.J., Jakoby, W.B., J. Biol. Chem., 1974, 249, 7130.

[42] Cotton, F.A., Walton, R.A., Multiple Bonds Between Metal Atoms, 2nd ed., Clarendon Press., Oxford, 1993.

[43] Bear, J.L., Gray, H.B., Rainen, L., Chang, I.M., Howard, R., Serio, G., Kimball, A.P., Cancer Chemother. Rep., 1975, 59, 611.

[44] Hui, B.C.Y., Teo, W.K., Rempel, G.L., Inorg. Chem., 1973, 12, 757.

[45] Barbera, J., Esteruelas, M.A., Levelut, A.M., Oro, L.A., Serrano, J.L., Sola, E., Inorg. Chem., 1992, 31, 732.

[46] Isci, H., Mason, W.R., Inorg. Chem., 1985, 24, 1761.

[47] Barton, J.K., Rabinowitz, H.N., Szalda, D.J., Lippard, S.J., J. Am. Chem. Soc., 1977, 99, 2827.

[48] Barton, J.K., Rabinowitz, H.N., Szalda, D.J., Waszcak, J.V., Lippard, S.J., J. Am. Chem. Soc., 1979, 101, 1434.

[49] Lippert, B., Neugebauer, D., Raudaschl, G., Inorg. Chim. Acta, 1983, 78,161.

[50] Barton, J.K., Caravana, C., Lippard, S.J., J. Am. Chem. Soc., 1979, 101, 7269.

[51] Laurent, J.P., Lepage, P., Castan, P., Arrizabalaga, P., Inorg. Chim. Acta, 1982, 67, 31.

[52] Zaki, A.A., McAuliffe, C.A., Friedman, M.E., Hill, W.E., Kohl, H.H., Inorg. Chim. Acta, 1983, 69, 93.

[53] O'Halloran, T.V., Mascharak, P.K., Williams, I.D., Roberts, M.M., Lippard, S.J., J. Inorg. Chem., 1987, 26, 1261.

[54] Matsumoto, K., Urata, H., Chem. Lett., 1994, 307.

[55] Matsumoto, K., Sakai, K., Nishio, K., Tokisue, Y., Ito, R., Nishide, T., Shichi, Y., J. Am. Chem. Soc., 1992, 114, 8110.

[56] Matsumoto, K., Sakai, K., Nishio, K., Chem. Lett., 1991, 1081.

[57] Matsumoto, K., Watanabe. T., J. Am. Chem. Soc., 1986, 108, 1308.

[58] Lempers, E. L. M., Reedijk, J., Inorg. Chem., 1990, 29, 217.

[59] Yaman, Ş. Ö., Önal, A. M., Isci, H., Z. Naturforsch., 2001, 56, 202.

[60] Lund, H., Hammerich, O., Marcell Dekker Inc., 2001, 621.

[61] Borsan, M., Cannio, M., Gavioli, G., Electroanalysis, 2003, 15, 1192.

[62] Rauf, S., Gooding, J.J., Akhtar, K., Ghauri, M.A., Rahman, M., Anwar, M.A., Khalid, A.M., J. Pharm. Biomed. Anal., 2004, 34, 879.

[63] Erdem, A., Ozsoz, M., Electroanalysis, 2002, 14, 965.

[64] Boldron, C., Ross, S.A., Pitie, M., Meunier, B., Bioconjugate Chem., 2002, 13, 1013.

[65] Pitie, M., Burrows, C.J., Meunier, B., Nucleic Acid Res., 2000, 28, 4856.

[66] Bleckburn, G.M., Gait, M.N., Nucleic Acids in Chem. Biol., 1990, 297.

[67] Graves, D.E., Velea, L.M., Curr. Org. Chem., 2000, 4, 915.

[68] Duan, D., Pharmacology, 2004, 601, 61.

[69] Fox, K.R., Waring, M.J., Nucl. Acids Res., 1984, 12, 9271.

[70] Hadman, R.D., Skellern, G.G., Weigh, R.D., Nucl. Acids Res., 1998, 26, 3053.

[71] Kessler, H., Gehrke, M., Griesinger, C., Angew. Chem. Int. Edn. Engl., 1988, 27, 490.

[72] Powers, R., J. Struct. Func. Genom., 2002, 2, 113.

[73] Yamashita, M. Fenn, J.B., J. Phys. Chem., 1984, 88, 4451.

[74] Karas, M., Backmann, D., Bahr, U., Hillenkamp, F., Int. J. Mass Spectrom. Ion Process., 1987, 78, 53.

[75] Berkel, G.J.V., Eur. J. Mass Spectrom., 2003, 9, 539.

[76] Barber, M., Bordoli, R.S., Elliot, G.J., Sedgwick, R.N., Tayler, A.N., Anal. Chem., 1982, 54, 645.

[77] Mohan, J., Organic Spectroscopy, 2000, 351.

[78] TomLinson, A.J., Benson, L.M., Jhonson, K.L., Naylor, S., J. Chromatogr., 1993, 621, 239.

[79] Yoshitsigu, H., Fuhuhara, T., Ishibashi, M., Nanbo, T., Kagi, N., J. Mass Spectrom., 1994, 34, 1063.

[80] Gopal, M., Shahabuddin, M.S., Inamdar, S.R., Proc. Indian Acad. Sci., 2002, 114, 687.

[81] Morjani, H., Riou, J.F., Nabiev, I., Cancer Res., 1993, 53, 4784.

[82] Le Gal, J.M., Morjani, H., Cancer Res., 1993, 53, 3681.

[83] Caldwell, J., Kollman, P.A., Biopolimers, 1986, 25, 249.

[84] Cieplak, P., Rao, S.N., Biopolimers, 1990, 29, 717.

[85] Huang, Y.Q., Jiang, H.L., Luo, M.X., Acta Pharmacol, 2000, 21, 536.

[86] Delahoussaye, Y.M., Hay, M.P., Pruijn, F.B., Denny, W.A., Biochem. Pharmacol. 2003, 65, 1807.

[87] Bailly, C., Colson, P., Houssier, C., Nucl. Acids Res., 1996, 24, 1460.

[88] Houssier, C., Molecular Electro-Optics., 1981, 363.

[89] Bailly, C., Henichart, J.P., Colson, P., J. Mol. Recognit., 1992, 5, 155.

[90] Colson, P., Bailly, C., Houssier, C., Biophys. Chem., 1996, 58, 125.

[91] Eriksson, M., Norden, B., Meth. Enzymol, 2001, 340, 68.

[92] Guttman, A., Cooke, N., Anal. Chem., 1991, 63, 2038.

[93] Kraak, J.C., Bush, S., Poppe, H., J. Chromatogr. 1992, 680, 405.

[94] Heegard, N.H.H., J. Chromatogr., 1994, 680, 405.

[95] Hadman, I.I., Skellern, G.G., Waigh, R.D., Nucl. Acids Res., 1998, 26, 3053.

[96] Kemp, G., Biotechnol. Appl. Biochem., 1998, 27, 9.

[97] Jonsson, U., Malmquist, M., Adv. Biosens., 1992, 2, 291.

[98] Gambari, R., Curr. Med. Chem., 2001, 1, 277.

[99] Schuck, P., Annu. Rev., Biophys. Biomol. Struct., 1997, 26, 541.

[100] Merwe, V.D., Brown, P.A., Barclay, A.N., Trends Biochem. Sci., 1994, 19, 354.

[101] Barton, J.K., Danishefsky, A.T., Goldberg, J.M., J. Am. Chem. Soc., 1984, 106, 2172.

[102] Tysoe, S.A., Morgan, R.J., Baker, A.D., J. Phys. Chem., 1993, 97, 1707.

[103] Kelly, T.M., Tossi, A.B., McConnell, D.J., Strekas, T.C., Nucleic Acids Res., 1985, 13, 6017.

[104] Pasternack, R.F., Gibbs, E.J., Villafranca, J.J., Biochemistry, 1983, 22, 2406.

[105] Liu, J., Zhang, T., Lu, T., Qu, L., Zhou, H., Zhang, Q., Ji, L., J. Of Inorg. Biochem., 2002, 91, 269.

[106] Tabassum, S., Rarveen, S., Arjmand, F., Actabiomaterial, 2005, 1, 677.

[107] Suzen, S., Demircigil, B.T., Ozkan, S.A., New J. Chem., 2003, 6, 1007.

[108] Kauffmann, J.M., Vire, J.C., Anal. Chim. Acta, 1993, 173, 329.

[109] Wang, J., Cai, X., Rivas, G., Shraishi, H., Biosens. Bioelectron, 1997, 12, 587.

[110] Kissinger, P.T., J. Chem. Educ., 1983, 60, 702.

[111] Laviron, E., Electroanalytical Chem., 1982, 53.

[112] Nagy, Z., Modern Aspects of Elect., 1990, 237.

[113] Bond, A.M., Modern Polar. Meth. In Anal. Chem., 1980, 269.

[114] Brett, C.M.A., Elect. Principles., 1993, 208.

[115] Erdem, A., Ozsos, M., Electroanalysis, 2002, 14, 965.

[116] Hirohama, T., Kuranuki, Y., Ebina, E., J. of Inorg. Biochem., 2005, 99, 1205.

[117] Srinivasan, S., Annaraj, J., Athappan, P.R., J. of Inorg. Biochem., 2005, 99, 876.

[118] Mahadevan, S., Palaniandavar, M., Inorg. Chim. Acta, 1997, 254, 291.

[119] Carter, M.T., Rodriguez, M., Bard, A.J., J. Am. Chem. Soc., 1989, 111, 8901.

[120] Vaidyanathan, V.G., Balachandran, U.N., Royal Soc. Of Chem., 2005, 2842.

[121] Tew, K.D., Picket, C.B., Mantle, T.J., Mannervik, B., Hayes, J.D., Structure and Function of Glutathione Transferases, 1993.

[122] Landi, S., Mutation Research, 2000, 463, 247.

[123] Kearns, P.R., Hall, A.G., DDT., 1998, 3, 113.

[124] Daniel, V., Crit. Rev. Biochem and Mol. Biol., 1993, 3, 173.

[125] Yaman, Ş.Ö., Önal, A.M., Isci, H., Zeitschrift für Naturforschung, 2003, 58b, 563.